



## ISSUE 1/2015

### **Title Story // CAE-based parametric studies by process integration and automation**

Optimization of a dry block calibrator

Multi-body simulation of truck mountings

FE-simulation of turbocharger blades

Optimization of car window mechanisms

Verification of bolted connections of a combustion chamber

# RDO-JOURNAL

optiSLang

multiPlas

ETK

SoS



# PROCESS INTEGRATION AND AUTOMATION – KEYS FOR SUCCESSFUL VIRTUAL PRODUCT DEVELOPMENT

To stay competitive on the international market, production cycles have to be highly efficient. Often, there are conflicting goals regarding quality aspects, product robustness, production cost and time to market that have to be considered and solved. CAE-based Robust Design Optimization (RDO) is able to meet these challenges. If implemented as early as possible in the virtual prototyping, parametric studies help to economize hardware tests, to accelerate product development processes and to secure design performance.

In this context, the interactive integration of the participating CAD/CAE-processes is essential for collecting all available data and simulation results for an efficient workflow of product development. The challenge is to tighten the processes and to combine all disciplines. This can be achieved by using one collective hub to build up an automatable multi-disciplinary procedure. Thus, the concept and development phase can be secured by a standardized workflow with “built-in” quality assurance.

To fulfill these requirements, in optiSLang, the user is able to connect complex simulation processes of major CAE solvers as well as pre- and postprocessors in heterogeneous networks or clusters via an intuitive graphical user interface. The software provides the user with a wide range of direct access to parametric modeling CAE environments like ANSYS or SimulationX as well as to programming environments like EXCEL, MATLAB or Python. For ASCII file based design parametric definition, optiSLang offers an automatized localization of input parameters. The extraction of result values, for example, scalar, vector or signal outputs is supported via the Extraction Tool Kit (ETK). Thus, all methods of CAE-based sensitivity analysis, optimization and robustness evaluation can be comfortably approached. For further automation, the setup of best practice procedures and the selection of the most appropriate algorithms is guided and supported by wizards and default settings.

In ANSYS Workbench, which has become known as one of the most powerful parametric modeling environments, optiSLang’s parametric studies can be fully integrated with the version “optiSLang inside ANSYS”. An alternative for the integration of ANSYS Workbench projects into optiSLang CAD/CAE workflows is the ANSYS integration node. Furthermore, optiSLang supports ANSYS HPC Parametric Pack Licensing and simultaneous solving functionality to speed up the simulation process.

In the title story of this issue, it will be described in detail how optiSLang is used to implement an automated CAE-based procedure that satisfies the future needs of product development processes.

Apart from that, we again have selected case studies and customer stories about CAE-based Robust Design Optimization (RDO) applied in different industries.

I hope you will enjoy reading our magazine.

Yours sincerely



Johannes Will  
Managing Director DYNARDO GmbH

Weimar, June 2015

## CONTENT

**2 // TITLE STORY // INTEGRATION & AUTOMATION**  
CAE-based parametric studies by process integration and automation

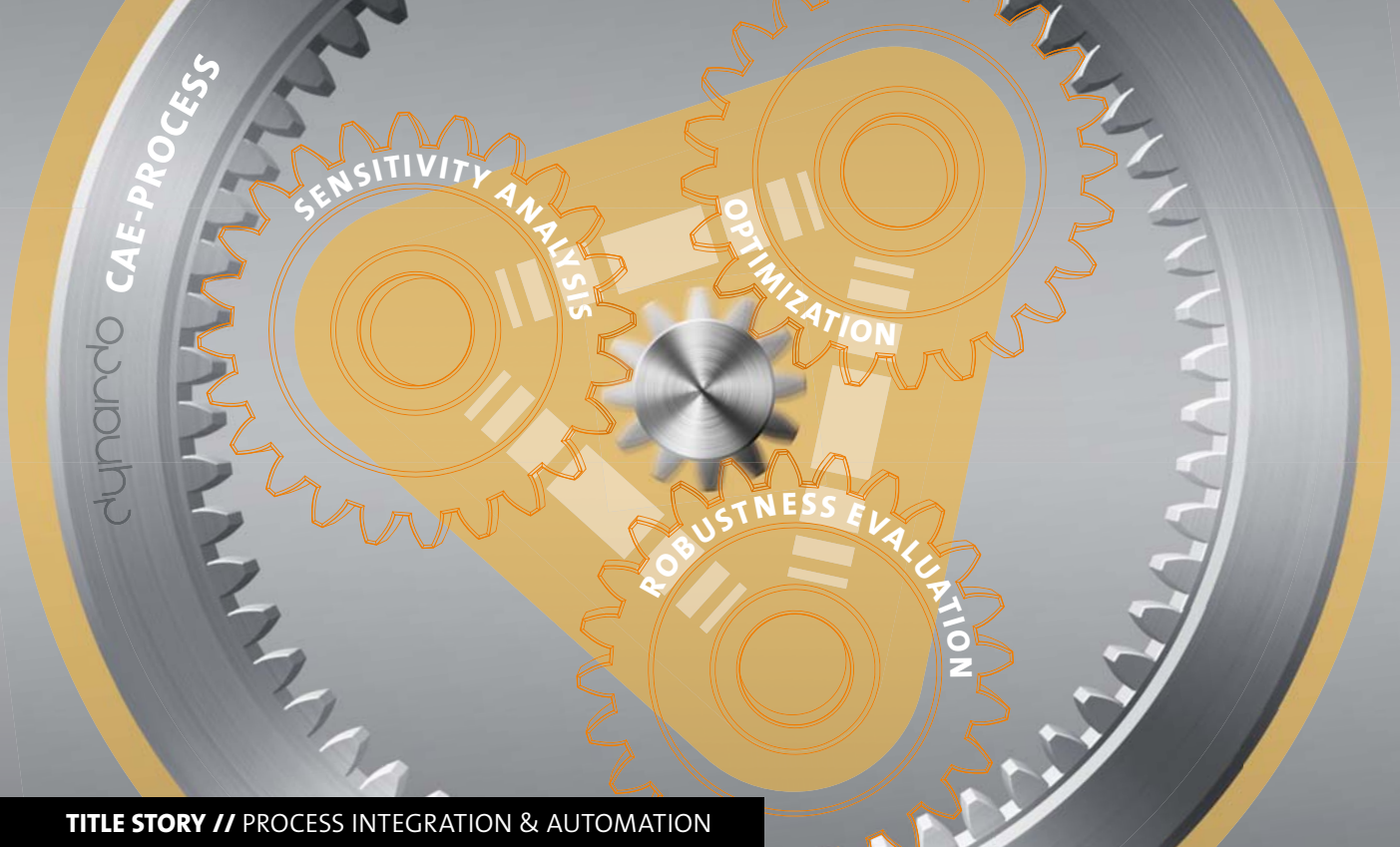
**8 // CASE STUDY // PROCESS ENGINEERING**  
Optimization of a multiple fixed-point cell as a reference in a dry block calibrator

**10 // CUSTOMER STORY // AUTOMOTIVE ENGINEERING**  
Multi-body simulation of truck mountings on rough road conditions

**16 // CUSTOMER STORY // TURBO MACHINERY**  
FE-model generation of turbocharger blades regarding geometrical tolerances

**22 // CUSTOMER STORY // AUTOMOTIVE ENGINEERING**  
Robust Design Optimization ensures high-quality window mechanisms

**25 // CUSTOMER STORY // AEROSPACE INDUSTRY**  
Fatigue verification of high loaded bolts of a rocket combustion chamber



TITLE STORY // PROCESS INTEGRATION & AUTOMATION

## CAE-BASED PARAMETRIC STUDIES BY PROCESS INTEGRATION AND AUTOMATION

optiSlang supports generation of automated CAE workflows in order to provide the full capabilities of Robust Design Optimization (RDO) for a competitive product development.

### What will be the most important features of product development processes in the future?

There are a lot of key words dealing with the enhancement of production processes like the Internet of Things or Production 4.0. However, in the end, it all comes down to a single point: to stay competitive on the international market where the most important issue is delivering better products. Here, “better” does not only concern features, it also aims at better quality. Additionally, customers ask for more enhancements in less time. To solve these requirements, production cycles are getting shorter and shorter. In addition, conflicting goals regarding quality aspects, product robustness, production cost and time to market have to be considered. In the classical product development processes (PDP), this problem was solved by using more resources. Now, we are faced with goods which have such a high complexity that even extensive development teams cannot control them anymore. To couple these facts with the requirement of product optimization, a new philosophy in the development process has to be established. Dynardo provides a procedure, called CAE-based RDO, which meets these challenges. Thus, it is possible to accelerate PDP as well as to introduce optimization strategies and “built-in” quality management.

Regarding this issue, different approaches exist like V (W, X, Y) – models, Kaizen or DMAIC circles. They all have two things in common. First, they state the necessity to connect all parts of the production cycle. Intended or unintended, a lot of companies have already implemented this strategy. Engineers and designers dealing with early production phases have to communicate with sales and support departments and vice versa. This principle is applied to all stages of the PDP. Secondly, the product development is not a straight one way road but needs to be thought and lived in circles of communication. Nowadays, the aim is to improve the product regarding weight, NVH or resource efficiency. Furthermore, the end user also expects a creative design. For that reason, PDPs have to be considered as early as possible in the development process.

### How can these concepts be transferred to real world usage?

The approach mentioned above illustrates a theoretical philosophy. To reach a benefit, it has to be applied to real processes. This can be economically accomplished when the philosophy is applied to a technical part or constraint. From Dynardo’s point of view, this can only be achieved if

the techniques are “built-in”. Everyone in the PDP-cycle has a strategy to solve a given task. No one starts from the very beginning. There is personal experience and education regarding tools and established processes. And even personal preferences have to be taken into account. It cannot be the aim to force all participants to throw away their solutions and forget about valuable experiences.

The best way to address these boundary conditions is using the principle itself. Implementing the approach should be an interactive cycle. Thus, “the way to the better” (Japanese for Kaizen) can be found. This way is the most economical one and guarantees success. Each part of the PDP can define its own improvement pace. In fact, the existing processes have to simply be connected. Therefore, it would be helpful if all involved specialists have access to a single collective hub where they can share their knowledge and skills. The benefit of this teamwork is evident.

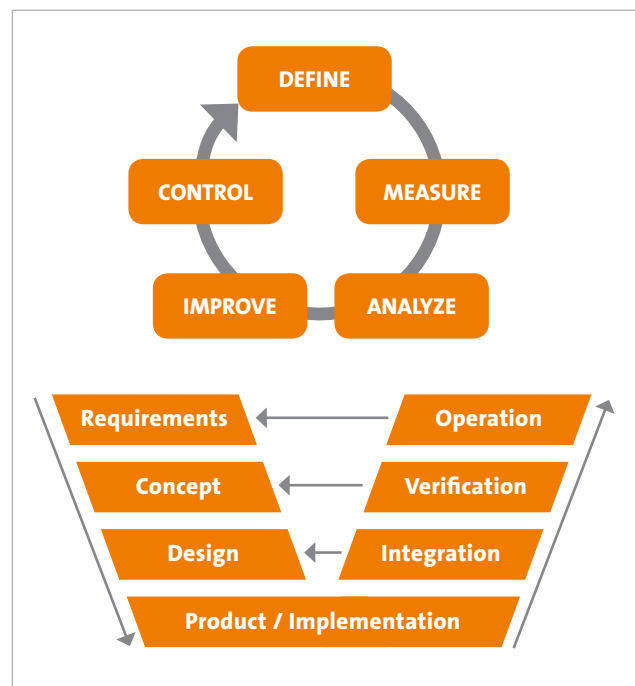
In the following, it will be described in detail how the concepts can be transferred into a continuous improvement procedure that satisfies the future needs of product development processes. These issues will be addressed:

- Techniques to get better products
- Connection of all necessary CAD/CAE Tools
- Answers how these tools can be combined
- Generation of a platform for collaborative work

### Virtual product development and multiple disciplines

As the product cycles are continuing to get shorter and requirements are rising, complex and expensive hardware tests need to be replaced at least partially by CAD, CAE or CAM. Regarding the “rule of ten”, as a strategy for resolutions of measurement systems, those techniques need to be used in early production phases. Using this technique is common and necessary to be competitive on the international market. Here, the engineer has the most intervention options at a comparatively low cost level. Virtual product development using the power of simulation needs to be introduced. In the meaning of the “cycle concept”, the usage of Virtual PDP (VPDP) needs to be extended. Hardware tests still capture an extensive part of the modern product development. Of course, CAD-based product designs need to be validated in the real world. Here, data from the production line is the input for products of the next generation. How test engineers are involved in this concept will be illustrated later in this article.

A product idea mostly starts with a drawing and makes CAD (Catia, Creo, Nx, Solidworks etc.) an appropriate starting point of virtual product development. Once a design is created, a structural analysis can use the model for meshing and solving. To obtain the best information about the design performance, the CAD model needs to be as realistic as possible. At



the same time, because of restricted computation power, the simulation model also has to be simplified. Therefore, many CAD tools or extensions exist for defeaturing purposes. They simplify the simulation model while keeping the original CAD untouched. An expert decides which detail level has to be chosen. This decision can be part of an automatized workflow. If different scenarios or load cases are defined, they are all applied to the same geometry. To consider all disciplines, more influences have to be included. Beside structural constraints, a product needs to satisfy e.g. economic requirements as well. These can be considered by implementing standard tools like MS Excel into the automated workflow. To summarize, the results need to be communicated and discussed. As a consequence, all data can be collected and processed as well as meaningful reports can be created automatically.

The challenge now is to tighten the processes and to combine all disciplines. This can be achieved by using one collective hub to build an automatable multi-disciplinary process. Thus, a designed concept can be proven through calculation. If all of these disciplines are connected in a standardized workflow, the designer can evaluate the concept by some mouse clicks. Through the described automation, the virtual product development receives a standardization. A “built-in” quality assurance is inherited by the whole VPDP.

### Parametric studies

Once a standardized and automatable workflow is set up, it can be used for parametric studies to:

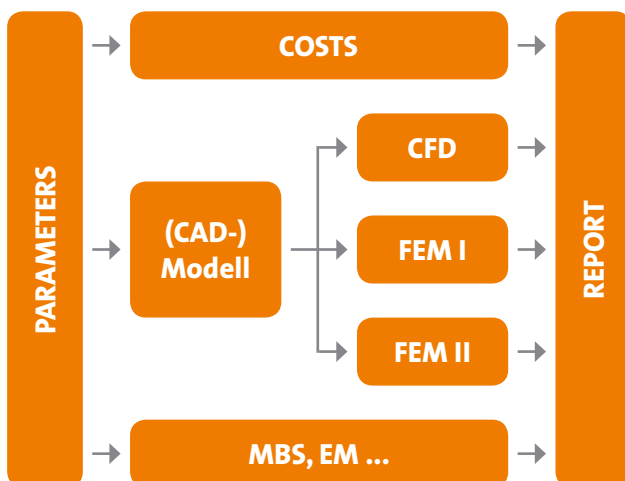
- Understand the design by conducting a sensitivity analysis
- Improve the design by using methods of optimization
- Validate the quality of the design by conducting a stochastic analysis



There are several solutions for parametric studies delivered within CAE codes. One example is the ANSYS Workbench. Here, parametric CAD and CAE can be connected to one complete multi-physics simulation workflow. ANSYS Workbench established a powerful parametric modeling environment including interfaces to major CAD programs in order to secure the availability and generation of suitable CAE parametric models as a key requirement. It has the capability to collect CAE and CAD data in a central parameter manager. Consequently, the system integration, process automation and job control are also integrated into ANSYS Workbench to update one or multiple designs from the parameter manager.

Other solutions can be found, for example, in AMESim, FloEFD, Friendship Framework or Zemax. They all support the replacement of numeric values for parametric models of the underlying CAE process. This is combined with an automatized update of the model. Usually, this functionality is very powerful and generally usable as well as it supports HPC and simultaneous solving. But mostly there is a lack of connection to include other tools which are used in VPDP. Consequently, the provided algorithms for studies, the possibilities to define input parameters and the definition of observed outputs are limited to the common application fields of the solver. The majority of the VPDP software tools do not have an explicit parameter management system. In this list, very common codes like Matlab and special solutions like “in-house” tools can be found.

To overcome all of the mentioned constrictions, interfaces are provided to be used by process integration solutions. Different parametric environments can be collected and combined to one automatized parametric workflow for the modern product development. This software for process integration is the needed collective hub.



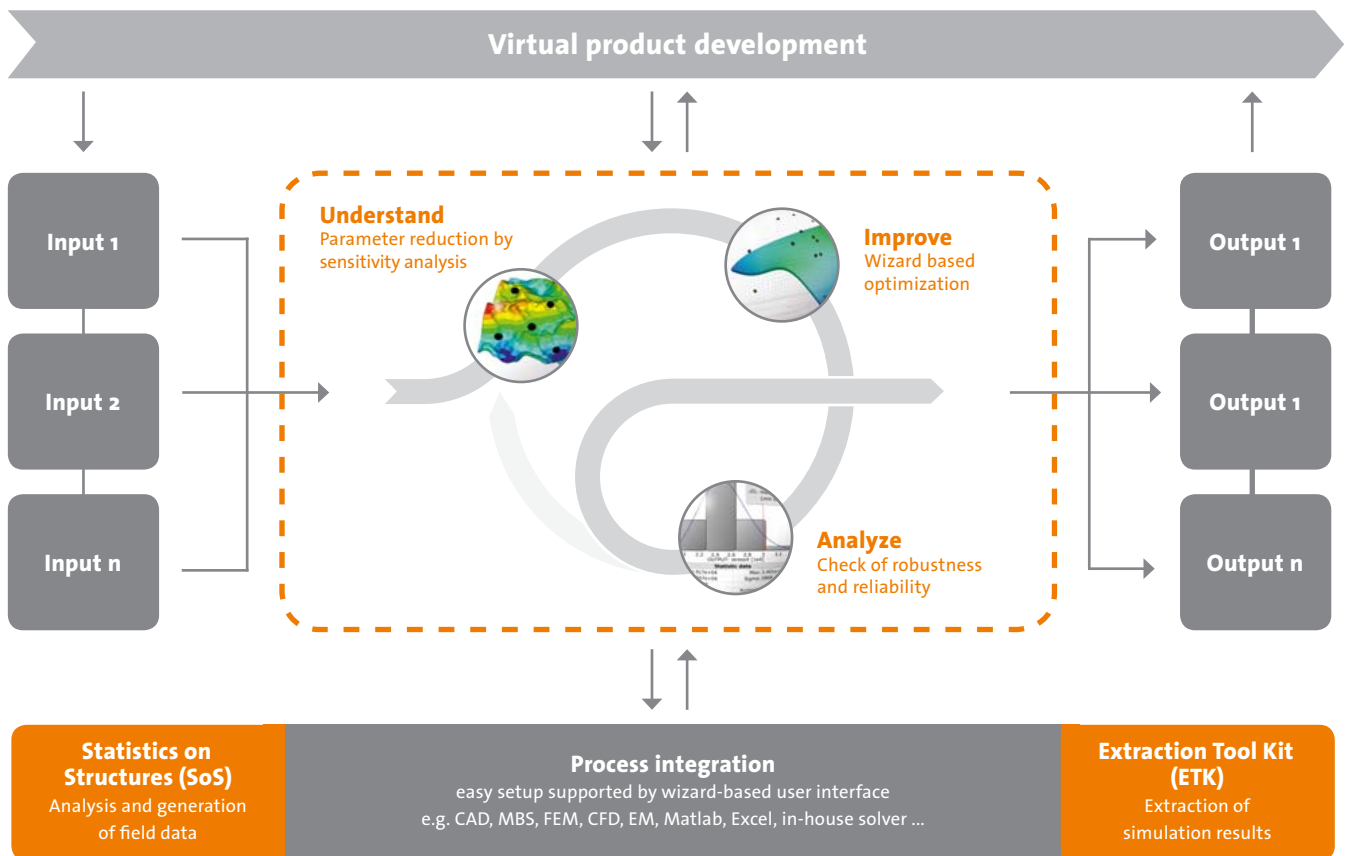
### optiSLang

optiSLang is Dynardo’s software for CAE-based sensitivity analysis, multi-objective and multi-disciplinary optimization, robustness evaluation, reliability analysis and Robust Design Optimization. In order to implement the described cycle concepts, optiSLang’s former C/Fortran backbone of the interpreter language was transformed into modern modular C++ with Python bindings. This could be managed without rewriting all successful parts of the existing powerful algorithms. New algorithmic implementations, the toolbox for nature-inspired optimizers and improvements of the MOP were developed in C++ modules. Additionally, Dynardo already had a decade of scripting experiences in supporting HPC and automatizing CAE. This valuable knowledge was used to develop a new kernel for the workflow setup. The task was to replace the main part of the scripting solutions by more convenient elements. The development of the post processing tool ETK (Extraction Tool Kit) was also a very important step in the improvement cycle. Users of supported formats, e.g. Abaqus, had the opportunity to benefit from better assistance to parametrize and appraise responses. In 2012, version 4 was released with a new GUI and kernel.

### Tool integrations and collaborative work

optiSLang’s GUI supports the interfacing to almost any software tool which is used in VPDP and fulfills the requirements to run in batch or to except parameter variation. The interfaces are mainly used “inside optiSLang”. Thus, in optiSLang context, they are called “tool integrations”. Many different VPDP software solutions are coupled with optiSLang. They are automatized either in a single solver process chain or in very complex multi-disciplinary and multi-domain workflows. Even performance maps and their appraisal can be part of standardized projects. The new generation of optiSLang provides direct access to the parametric modeling of CAE environments like ANSYS or SimulationX as well as to programming environments like EXCEL, MATLAB or Python. It allows users to combine several tools in sequences and iteration loops. For a constant workflow control, failed designs due to missing licenses, geometries unable to be meshed or any other inconsistency is secured. Here, the workflow stores the usable data for further execution. Of course, the support of different platforms, i.e. Windows, Linux and HPC as well as Cloud computing is provided. Thus, optiSLang is the solution to automatize VPDP.

All of the previously described workflows can be stored as reusable templates and made available for the entire VPDP team. Working this way guarantees the capturing of knowledge of each expert in the team. Every template is a version controlled building block. It can be used in a modular and flexible way within adaptive projects. While each expert

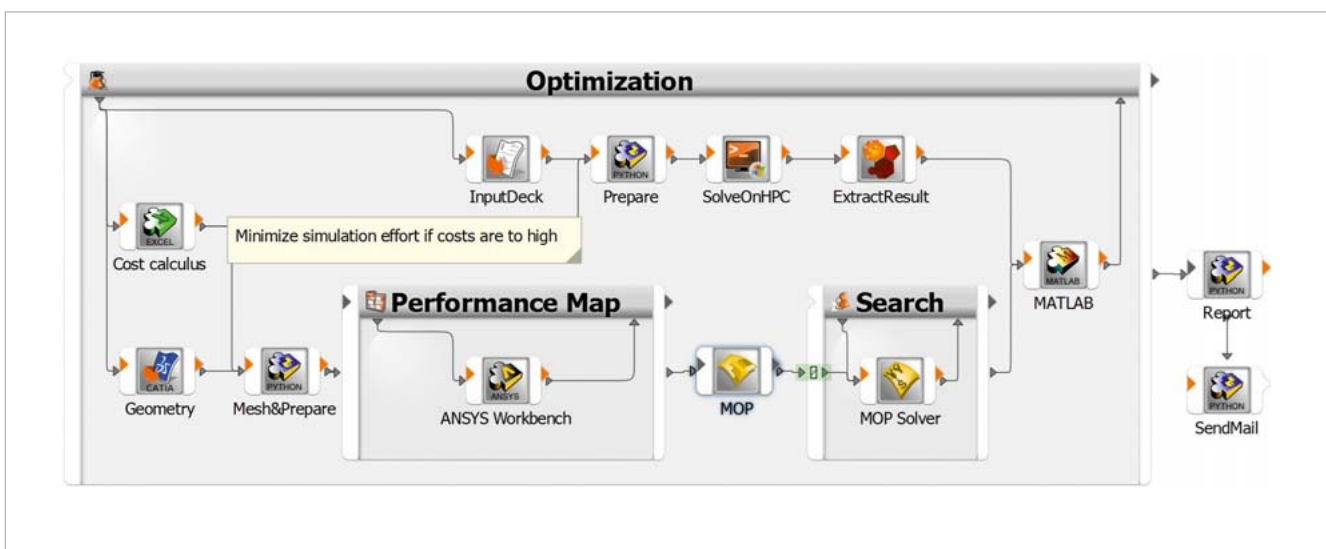


delivers quality assured sub-modules, the whole process becomes standardized. Used tools, algorithms and internal processes can be improved or changed while the entire PDP is stable and benefits from sub-upgrades. At the end, the whole team benefits from sharing knowledge in standardized processes by having quality assured PDP and has more time to focus on their following improvement steps for the process itself or for the product. Through the modular approach, the necessary flexibility to create modern and innovative products is guaranteed. The concept also assures collaborative,

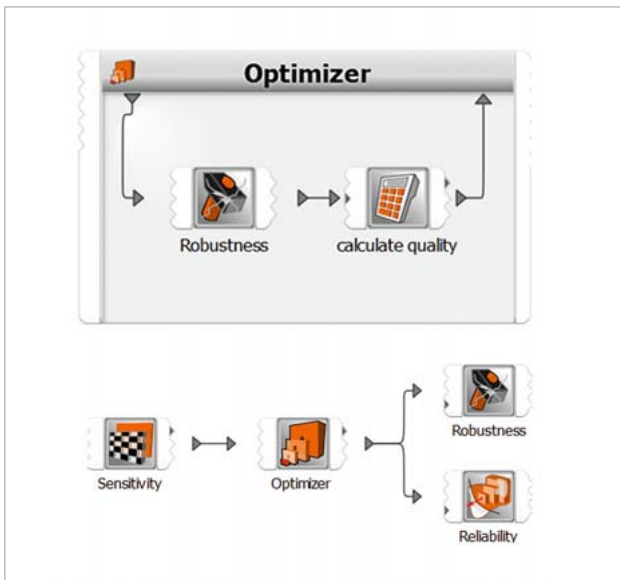
flexible and standardized work. Thus, optiSLang is the platform for efficient, future oriented teamwork.

### Workflows for CAE-based Robust Design Optimization

- optiSLang provides algorithmic building blocks for
- Sensitivity Analysis and MOP
  - Multi-objective and multi-disciplinary optimization
  - Robustness evaluation



Fully automatized optimization workflow in optiSLang considering structural costs and metric of performance map, running several solvers and using HPC



Workflows for coupled and iterative RDO

All of the algorithmic modules can be used as a single system. They can also be combined in nested loops or complex sequential workflows. The setup of best practice procedures is guided and supported by wizards and default settings. Thus, with optiSLang, the generation of a workflow using the modules of sensitivity analysis, optimization and robustness evaluation is possible with a minimum of user input. A best practice management chooses, according to the RDO task, an optimization strategy with the most fitting and effective algorithms.

The graphical user interface supports the workflow approach visually. Single building blocks and algorithms are graphically coupled in order to show dependencies and scheduling. The relationships can be determined and controlled in one context. Easily understandable charts as well as control panels are displayed at the same time. This enables full access and traceability of the complete workflow. Conducting a sensitivity analysis, multidisciplinary optimization, robustness evaluation and reliability analysis with optiSLang enables you to:

- Quantify risks
- Identify optimization potential
- Improve product performance
- Secure resource-efficiency
- Save time to market

### Interfaces and Extensibility

As stated before, openness of VPDP software tools is an important property. It enables the tool to integrate or to be integrated into other PDP environments. To fulfill these requirements, optiSLang provides several interfaces. The provided Python, C++ and command line interfaces allow the automatic creation, modification and execution of projects.

For that reason, the usage within custom applications, e.g. PLM/SPDM systems, is secured. In PLM systems like Teamcenter, the team members can share their knowledge and use the work of others mutually. CAD models, simulation, workflows, product information and results can be managed in those systems. Through a flexible interface optiSLang supports commercial tools as well as versioning systems like subversion or even in-house solutions. This guarantees full consistency and traceability of PDP.

Additionally, optiSLang projects can be integrated into customized platforms. Repetitive and exhausting tasks can be standardized and automatized. One goal of these techniques is to provide standardized forms with a minimum of needed input to the rest of the team. Thus, even non CAE experts can become able to use the benefits of CAE-based simulation and generate optimal and reliable designs. A lot of successful implementations of optiSLang into company solutions were realized over the last years. Even fully automatized RDO workflows were generated. This enabled the establishment of company-wide standards in virtual product development. Hence the customer benefits from consistent and efficient processes.

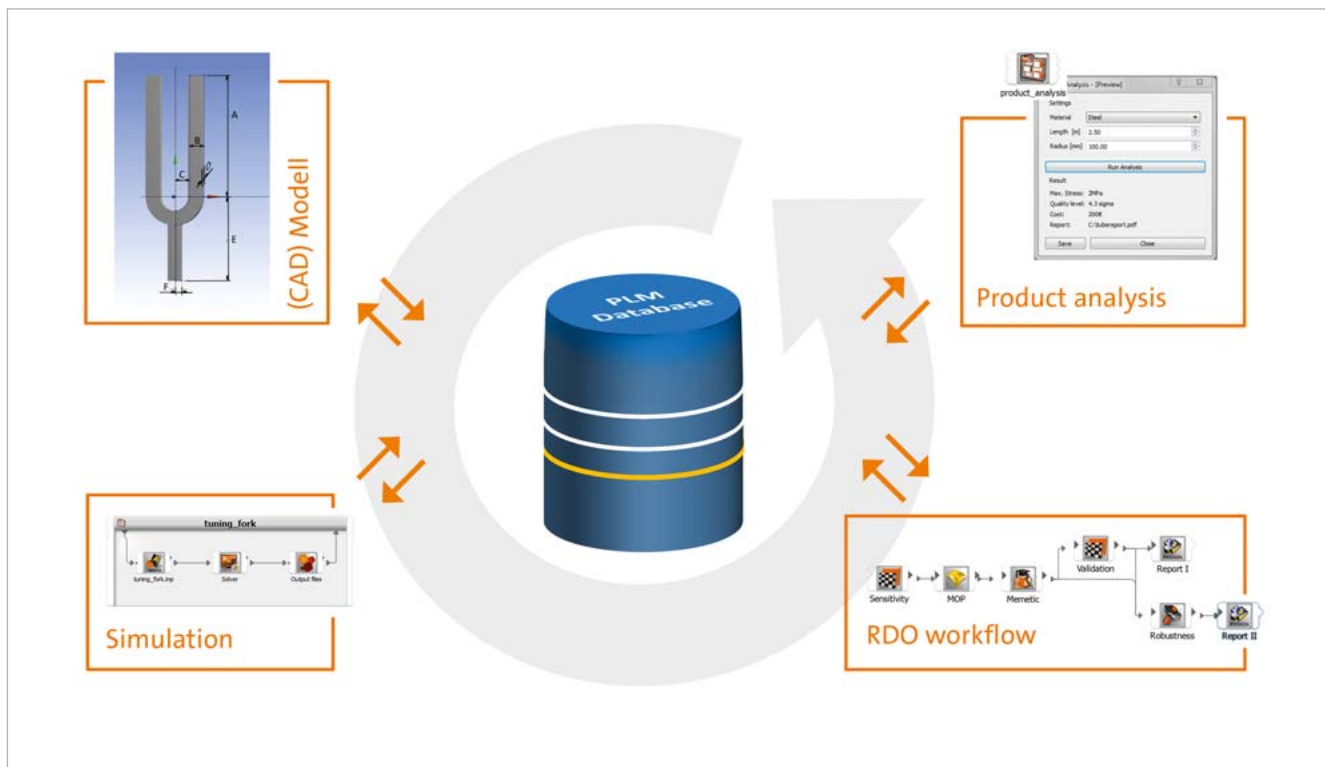
The openness of Dynardo's software optiSLang also provides users with a plug-in for their own:

- Algorithms for DOE, Optimization, Robustness etc.
- Meta models
- Tool integrations

Current requirements for flexibility and upcoming requests for extensibility are satisfied by those interfaces. Thus, optiSLang is the platform to address future needs of PDP.

### optiSLang inside ANSYS

ANSYS provides a customization toolkit for its Workbench. It can be used to extend its functionality. Based on this idea, a direct integration of optiSLang into the parametric modeling environment of ANSYS Workbench was developed to make optiSLang's state of the art RDO workflows available in this standard CAE environment. It can be accessed through a minimized user input and wizard guidance. The Workbench functionality was also broadened by optiSLang's signal processing integration. Users are able to implement responses which are not extractable or integrated in standard ANSYS Workbench, e.g. non-scalar responses like load displacement curves. Non scalar responses can be considered, for example, in parameter identification or optimization. If all parameters and needed VPDP tools are available in the Workbench parameter manager, optiSLang inside ANSYS is a useful integration mode. Alternatively, for integration of ANSYS Workbench projects in optiSLang, an integration node is available. This mode is recommended to be used for solving VPDP tasks which need additional parameters or for CAE-integration not yet provided inside ANSYS.



Scene of a modern Product Development Process using collaborative work based on a PLM / SPDM data base and optiSLang

### optiSLang Excel Add-in

Using its interfacing capabilities, MS Excel and optiSLang work together to support PDP. With the help of the Excel Add-in, external data, e.g. from hardware measurement, can be converted into optiSLang compatible formats. Consequently, the data from laboratories can be directly forwarded to sophisticated algorithms like optiSLang's Metamodel of Optimal Prognosis (MOP) and important coherences can be mined, visualized as well as extracted as functions. Thus, the first target of Robust Design can be addressed: A Better Design Understanding. Based on transferred observations, meta models are built and hard-ware tests can be replaced by those surrogates. While forwarding measurement data and applying standardized evaluation methods, the laboratory engineer can be integrated into the complete VPDP.

### Conclusion

Finally, after discussing requirements and solutions, the following main preconditions of a successful product development processes in the future can be summarized:

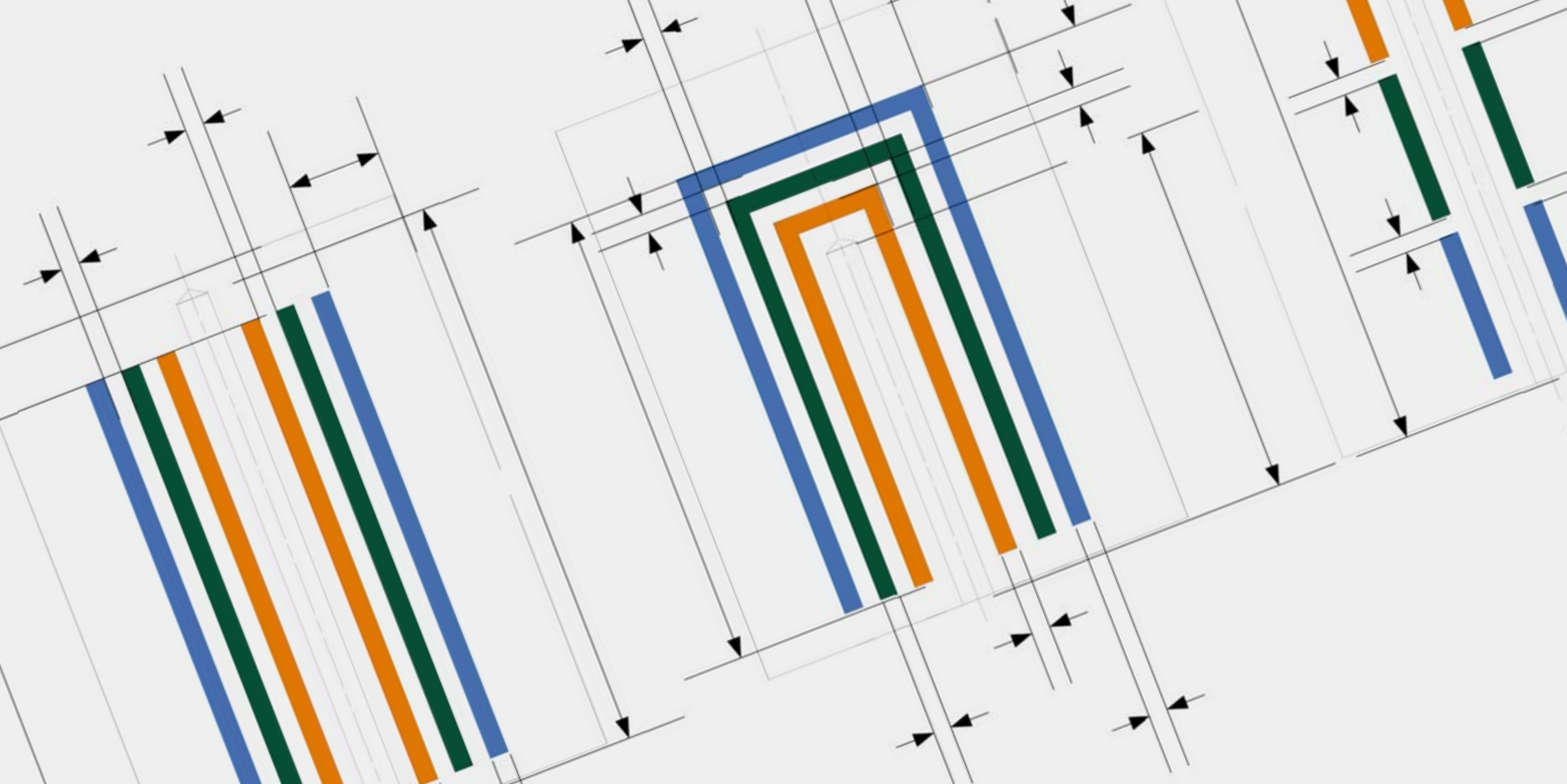
- Automation and standardization of VPDP workflows
- Parametric studies and Robust Design Optimization
- Flexibility and extensibility
- Support of continuous improvement
- Enabling of collaborative work

As explained in this article, optiSLang fulfills all of these requirements. Using the software, existing flows can be im-

plemented or standardized. The software package provides solutions for all phases of PDP. The fulfillment of future requirements and a continuous process of improvement are secured by modular and flexible concepts. Traceability and quality assurance are technically seized. The inherent usage of parametric studies and RDO leads to a "built-in" improvement of the product.

As shown in this article, optiSLang guarantees a cost efficient and successful development of better products.

**Authors //** Dr. D. Schneider / H. Schwarz (Dynardo GmbH)



CASE STUDY // PROCESS ENGINEERING

## OPTIMIZATION OF A MULTIPLE FIXED-POINT CELL AS A REFERENCE IN A DRY BLOCK CALIBRATOR

The thermal and geometrical designs of a multiple fixed-point cell could be optimized for an improved in-situ calibration by means of optiSLang and thermal simulations in ANSYS.

### Introduction

Temperature sensors for industrial applications are usually calibrated by comparison with reference thermometers in thermostats or dry block calibrators. At the Institute for Process Measurement and Sensor Technology of the Technische Universität Ilmenau, a new dry block calibrator was designed with the aim of performing calibrations by comparison reaching an uncertainty less than the one currently reached with the existing dry block calibrators.

An important part of this novelty calibrator is the inclusion of a multiple fixed-point cell. Inside, it has three pure materials, indium ( $T_{ph}=156.5985^{\circ}\text{C}$ ), tin ( $T_{ph}=232.928^{\circ}\text{C}$ ) and zinc ( $T_{ph}=419.527^{\circ}\text{C}$ ), called fixed-point materials. They have their fixed-point temperature  $T_{ph}$  (Melting and Freezing temperature) within the work range of the dry block calibrator from  $20^{\circ}\text{C}$  to  $600^{\circ}\text{C}$ . These temperatures are reproducible with an uncertainty of some millikelvin and they are defined in the International Temperature Scale from 1990 (ITS-90). In the case of the dry block calibrator, the fixed-point materials allow an in-situ calibration of the block calibrator internal reference sensor at their phase change temperatures. Thus, the calibration values are traceable to the

ITS-90. The cell was designed by the Finite Element Method in ANSYS Workbench and optimized by parametrical variations in optiSLang.

### Geometrical Design

For the design of the multiple fixed-point cell, three different geometries with coaxial arrangement of the fixed-point materials were used as models. For each model, some geometrical parameters (a to h, Fig. 1), according to the calibrator's geometry were defined. The position of each material in the cell also varied (in, ctr, out, Fig. 1). Graphite was selected as the crucible material of the cell. This material is commonly used for the fixed-point cells due its high thermal conductivity, its chemical compatibility with the fixed-point materials and its good ability for the machining.

### Thermal Design

The main goal of the cell's design was to find a geometry and an arrangement of the fixed-point materials inside the cell having minimal thermal gradients in the cell and in the reference sensor during the change of a fixed-point material

p	Model 1			Model 2			Model 3		
	CoP %	iv	op	CoP %	iv	ov	CoP %	iv	ov
a / mm	28	23	13	6	23	20	14	13	25.3
e / mm	68	40	48.5	51	40	40	4	1	5
f / mm	5	5	3.25	9	5	3.25	47	15	4.9
i / mm	33	10	7	-	-	-	5	10	26.6
j / mm	-	-	-	-	-	-	5	3	1
in / °C	-	-	-	-	-	-	10	157	232
ctr / °C	5	232	232	2	-	-	10	232	157
out / °C	3	420	420	3	420	420	-	-	-
CoP fm / %	90			70			83		
ANSYS / mK	1620			1695			2562		
MOP / mK	1605			1803			2501		
rd / %	1			6			2		

Table 1: Selected geometrical and thermal parameters of each model after the sensitivity analysis with  $\Delta\vartheta T$  as an output parameter and optimization results with p as an input parameter, iv as an initial value, op as an optimized value, fm as a full model, rd as a relative difference

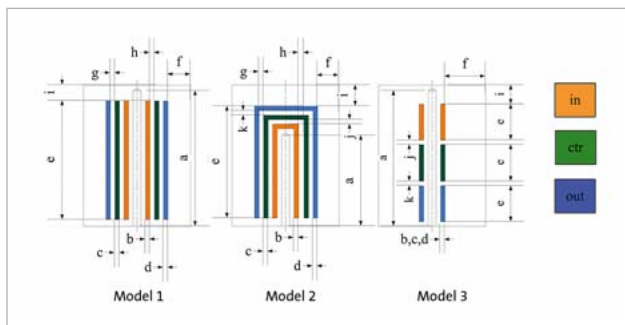


Fig. 1: Models with their fixed-point cell arrangements and parameters for the parametrical study

phase. In the ideal case, the reference sensor temperature is exactly the same as the phase change temperature of each fixed-point material. Focusing on this objective, static thermal simulations were made in three steps. In each step, it was assumed that every fixed-point material was at its fixed-point temperature, excluding the dry block calibrator, which was 2K over it. Initially, the input parameters were searched by conducting a sensitivity analysis. They have an influence on the output parameters that permit to estimate the quality of the temperature distribution, called  $\Delta\vartheta T$ . These output parameters were defined as the sum of the maximum temperature gradients in the cell for each phase change:

$$\Delta\vartheta_T = (\vartheta_{\max} - \vartheta_{\min})_T = (\vartheta_{\max} - \vartheta_{\min})_{In} + (\vartheta_{\max} - \vartheta_{\min})_{Sn} + (\vartheta_{\max} - \vartheta_{\min})_{Zn}$$

$\Delta\vartheta T$  = Sum of the maximal temperature difference on the cell for each fixed-point / °C |  $\vartheta_{\max}$  = Maximum temperature of the cell / °C |  $\vartheta_{\min}$  = Minimum temperature of the cell / °C

## Results

Table 1 shows the CoPs of the models and the input parameters which are relevant regarding the output parameter. It also shows initial and optimized values using an evolutionary algorithm. In addition, the calculated results in the MOP and in ANSYS, as well as their relative difference are shown. Here, it is possible to observe that a CoP of more than 70%

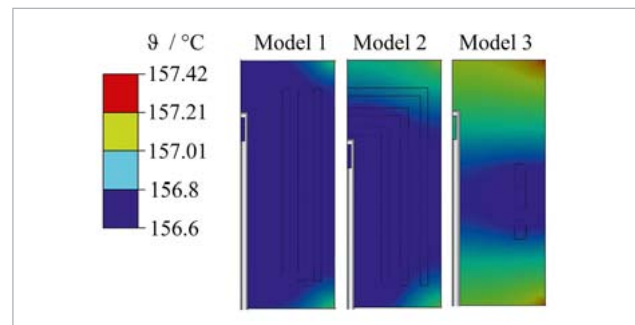


Fig. 2: Temperature field for the optimized models during indium's phase change

was enough to obtain a reliable result. After the optimization, it was discovered that model 1 of the multiple fixed-point cell was the best for the desired application. Fig. 2 shows the temperature distribution of the three models along with the phase change of Indium. It is possible to see that the temperature distribution for the model 1 is the most homogeneous. Similar results of temperature distributions were obtained for the phase changes of tin and zinc.

## Summary

A multiple fixed-point cell for an in-situ calibration of a new block calibrator's reference sensor was designed which is traceable to the ITS-90. This was possible by conducting finite element thermal simulations in ANSYS Workbench and a sensitivity analysis and optimization in optiSLang. The cell was designed with the aim to obtain the minimum thermal gradient during the phase changes of the fixed-point materials (In, Sn, Zn). An optimal cell's geometry and arrangement of the fixed-point materials inside could be found for this application.

**Authors //** S. Marin / Univ.-Prof. Dr.-Ing. habil. Th. Fröhlich (Institut für Prozessmess- und Sensortechnik, TU Ilmenau)

This material is based on the VIP-Project "TempKal" supported by the German Federal Ministry of Education and Research (BMBF).



CUSTOMER STORY // AUTOMOTIVE ENGINEERING

## MULTI-BODY SIMULATION OF TRUCK MOUNTINGS ON ROUGH ROAD CONDITIONS

**optiSLang enables a simulation of loads based on fast and cost-effective measurable signals for an efficient assessment of changes to the drivetrain configuration without the repetition of expensive driving tests.**

### Introduction

In the simulation of large mechanical systems such as full vehicle models, you have to retain the behavior of the interaction of multiple moving parts and also the behavior of complex force elements as simply as possible. In general, there are limits due to time and cost constraints, but above all, by the necessary parameterization of the many individual components of a system. One of the main difficulties in modelling is the reduction of the complex behavior of an individual component to its fundamental behavior without changing the overall behavior. The over-simplification of the force coupling elements leads to poor results of the simulation. The consequent necessary assessment and verification of the simulation results can be done via the comparison of the measured and simulated data.

The investigated MBS model is neglecting the elasticity of the supporting frame as well as the elasticity of all components of the drivetrain and it is reproduced by means of rigid bodies, which are connected by ideal joints and force elements. It is important to represent the properties of the main force coupling elements in sufficient detail, which is why the modelling of elastomeric bushings plays a special role. Due to its

material properties, the elastomeric bushing characteristics show a high scattering. Thus, they are ideal leverage points for a possible fine tuning in order to compensate previous model assumptions. Through careful selection of individual bushing model parameters and the use of nonlinear stiffness and damping characteristics, insufficient assumptions are partially compensated. In practice, parameter identification tools can take over the very time-consuming data input of the force coupling elements and optimize the result to a given target. In this context, the data input is now defined by means of comparison between the results of simulated and measured data as an optimization problem. The parameter identification of an MBS-submodel for the gearbox elastomer bushing enables the automated and optimized adjustment of the simulation with the measurement results. For this purpose, the elastomeric bushings of the engine and the gearbox are dynamically measured on a hydro-pulse test bench and these parameters are used as initial values in the process loop with the optimization software optiSLang and the multi-body simulation software Simpack. A frequency and amplitude-dependent elastomeric bushing model in Simpack is the necessary prerequisite for the examination of the dynamic behavior.

## Optimization process

In drive tests on rough roads, accelerations at individual points of the frame and the drivetrain are measured. From the measured accelerations, frame motion is calculated back to its rigid body motion in order to obtain real excitation signals for the frame in the simulation. In the multi-body simulation, this frame is specified as a motion function of time to finally obtain the simulated time behavior of the bushing forces and acceleration signals from the drivetrain.

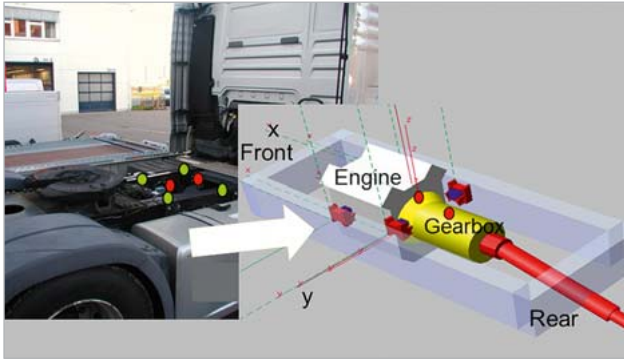


Fig. 1: MBS modelling | Green dots – acceleration sensors on the frame for calculation of the rigid excitation (input data for MBS simulation) | red dots – acceleration sensors for verification process (output data for MBS simulation)

To assess the quality of the simulated bushing forces, the model is verified by comparing the additionally measured acceleration signals on the engine and the gearbox from the driving test and the corresponding accelerations from the simulation.

By using suitable optimization software, you can automatize the process of ‘manual’ parameter search for the best possible correlation between measurement and simulation. In this case, the algorithm compares the results of the simulation with the detected rough road acceleration signals of the drivetrain and determines the deviation of the defined target function. To minimize the objective function, optiSLang differentiates between gradient method, response surface optimization (response surface methods) and stochastic search strategies.

The used algorithm ‘Adaptive Response Surface Method’ (ARSM) optimizes on the response surface of an approximation of the objective function. Pre-investigations have already shown that the parameter identification of elastomeric bushings for the complete test drive generates no satisfactory results. The challenging task is therefore to derive an optimization strategy that allows a separate consideration of the individual parts of the track for the extraction of individual parameters and characteristics. So, linear parameters have to be separated from nonlinear parameters through careful selection of individual maneuvers.

After completion of parameter identification, there must be a quantitative evaluation of the optimized result of the simulation with the measured values of the driving test. For this purpose, statistical methods are used. The calculation of the damage has proven to be a sensitive rating scale to represent a quantitative comparison of two curves. It is a pseudo-damage which is determined by assuming a ‘virtual’ fatigue life curve, so that the damage values allow relative comparisons.

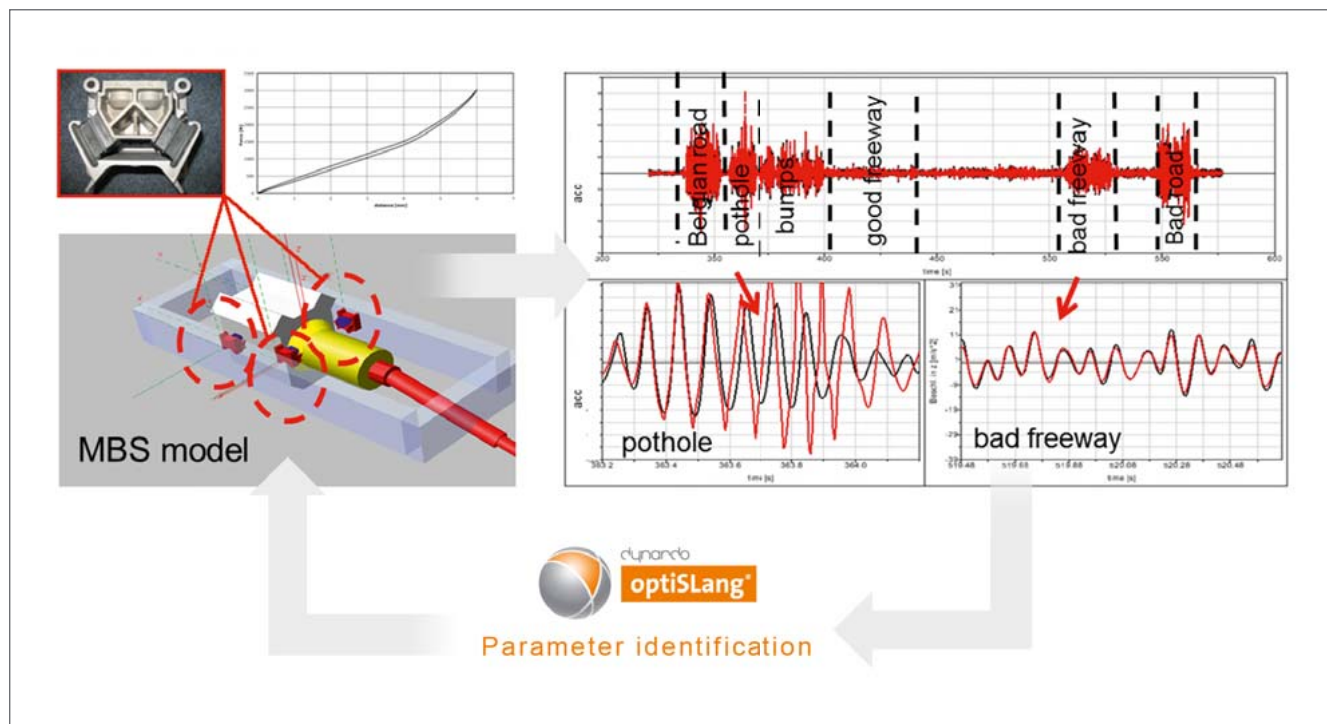


Fig. 2: Process loop of the identification process | black curves – measured acceleration signals = optimization target | red curves – simulation result of current optimization loop

### Derivation of the optimization strategy

The determination of good start design values is very important for the optimization process. Therefore, dynamically measured characteristics from a hydro-pulse test bench of engine and gearbox mounts were used. At the beginning, optimization experiments were started emanating from arbitrary start design values. Also, the attempt of the simultaneous identification of engine and gearbox mounts parameters did not yield a satisfactory result. Thus, the engine mount parameters were finally kept constant with the data input from the hydro-pulse measurement. Overall, many different variants of starting parameters (different stiffness model parameters, damping sizes, other model control variables, etc.) were tried out in order to identify early trends of positive result impacts.

In this context, the use of different optimization targets had a very large influence on the result. The method used at the beginning of the study of 'Euclidean norm' turned out to be ineffective in this case. Finally, the maximum and minimum ordinate, within predefined time ranges, so called slots, was used. Thus, the absolute values of the extreme value differences between simulation and measurement were added in the respective directions of the bushings and the optimization target was the minimization of the total value. Also, the use of two locally separated acceleration values on the

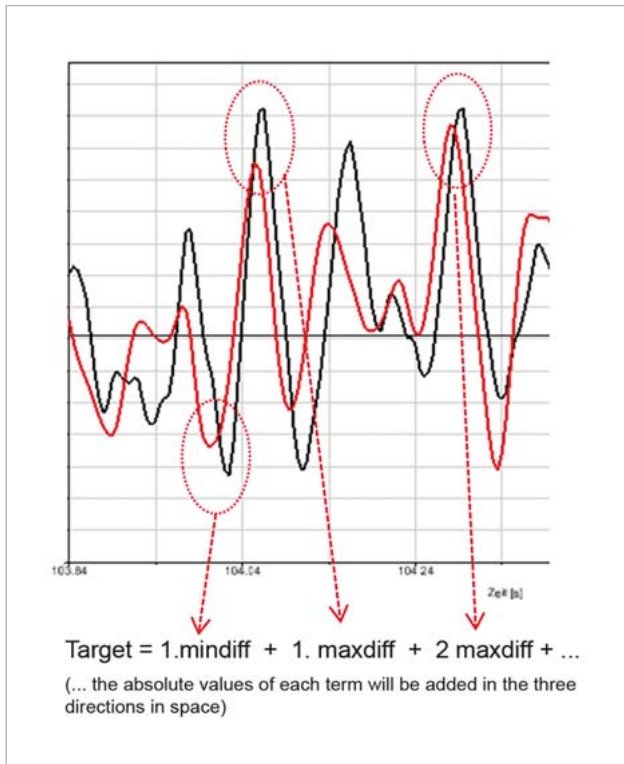


Fig. 3: Process loop of the identification process

drivetrain within the target size calculation was an important detail. Otherwise, the rigid body rotation of the drivetrain would not have been properly recognized. First, the bushing parameters of the three spatial directions could

be identified, each separated from one another. At the end, the optimization was done in all three spatial directions together with reduced parameter limits. The essential idea of the developed optimization strategy

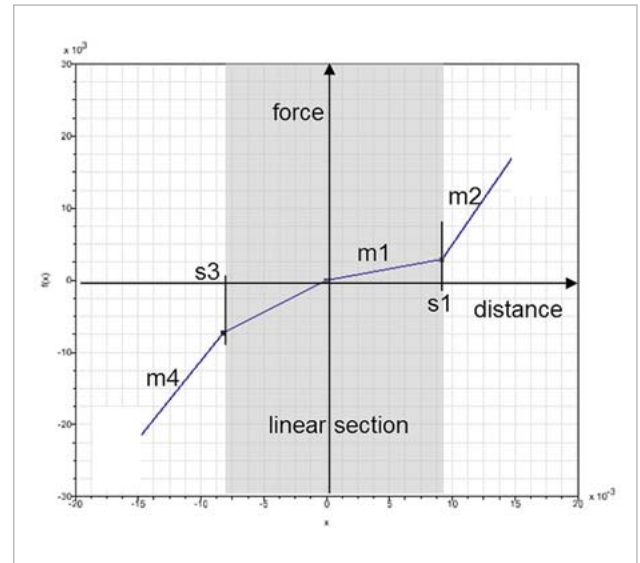


Fig. 4: Identification of stiffness characteristics

rested then on the assumption that there were sections of the complete track where only linear parts of the stiffness characteristics of the elastomeric bushings were loaded. Also, equal sections of the track were present where the

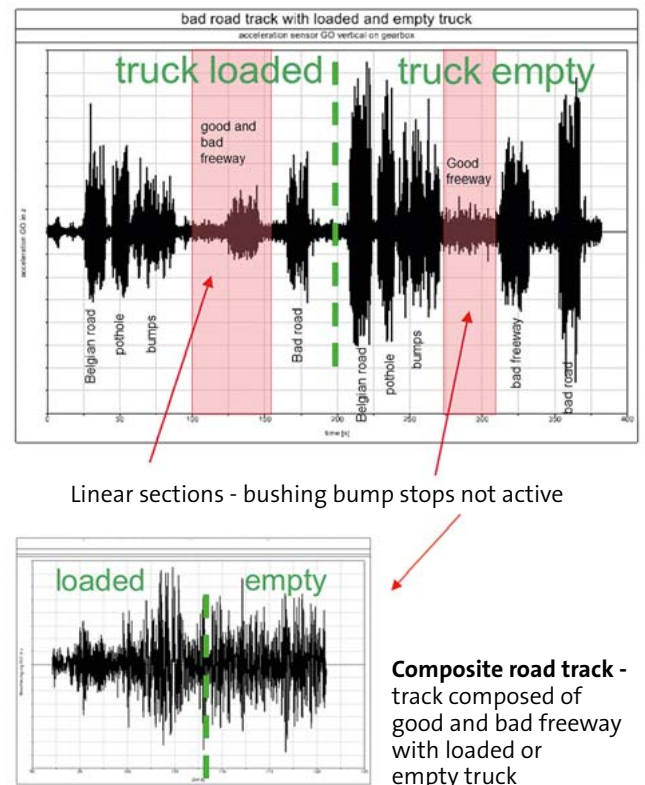
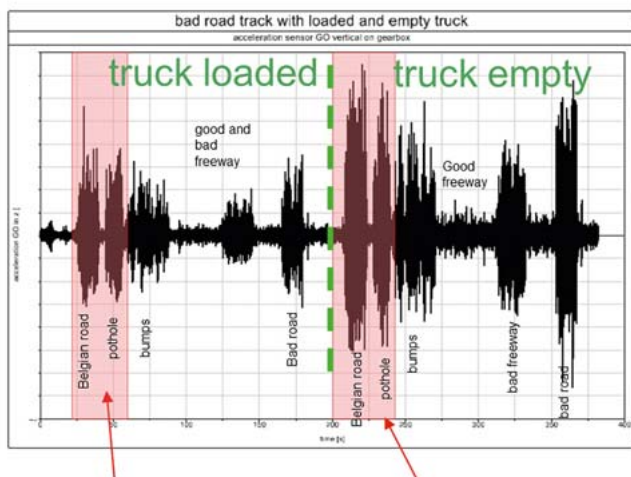


Fig. 5: Composition of linear sections

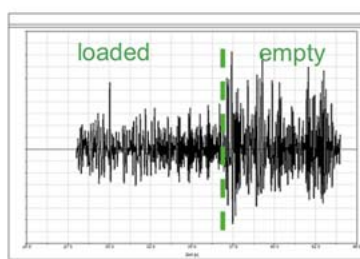
mounts operated in the nonlinear region of the stiffness characteristics. Such a process would be a response of the bump stops, which is implemented through the input of nonlinear stiffness characteristics. Creating such stiffness, a characteristics was achieved by identifying four parameters, which were respectively identified by the algorithm.

Sections that addressed only linear regions of the stiffness characteristics were considered as 'good' and 'bad' freeway. Here, the bump stops were not active. They were composed for the loaded and empty truck to a total 'linear section' of about 30 seconds duration.

The same procedure was applied to the areas where the bushings operated in the nonlinear regions of the stiffness characteristics, such as Belgian road and pothole track. Here, the largest amplitudes could be seen. The composed parts of the track had a time span of 15s.



Nonlinear sections - large amplitudes, bushing bump stops eventually active



Composite road track - track composed of belgian road and pothole sections with loaded and empty truck

Fig. 6: Composition of nonlinear sections

During the identification process of the non-linear parts of the bushing characteristics, the previously identified linear parameters of the bushing model were kept constant, so the individual identification loops were built on one another. A complete run of such an identification process took about 38 hours, with about 2700 calls of the MBS simulation. In order to keep the total time small, the duration of the composite sections for the MBS simulation should be kept as short as possible. During the total 8 process runs, the bushing param-

eters for the three spatial directions were first identified individually, then together and third also regarding the breakdown in linear and non-linear sections.

### Results

After the application of the derived optimization strategy in the separated identification process, the recalculation of the total track with the identified parameter from the linear and nonlinear sections was conducted. The diagram below shows the acceleration values of the sensor GO (gearbox above) in the three spatial directions (x, y horizontal lateral and z vertical).

The measured rough road accelerations were compared with the accelerations obtained from simulation.

- measured rough road accelerations (black)
- calculated accelerations (green) with the unchanged

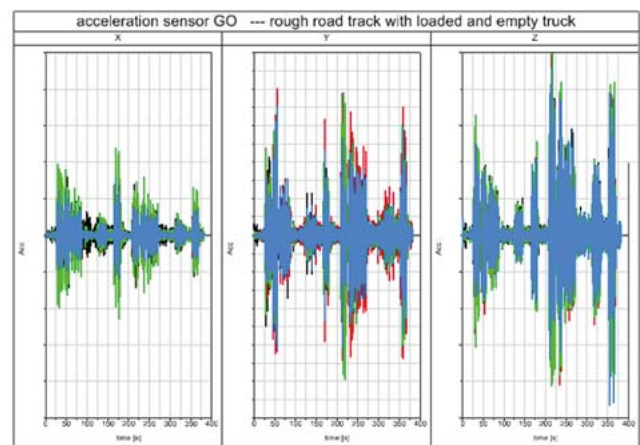


Fig. 7: Time history of acceleration data | black - measured data, green - simulated accelerations with dynamic measurements of the mounts, red - simulated accelerations after first optimization, blue - simulated accelerations after second optimization

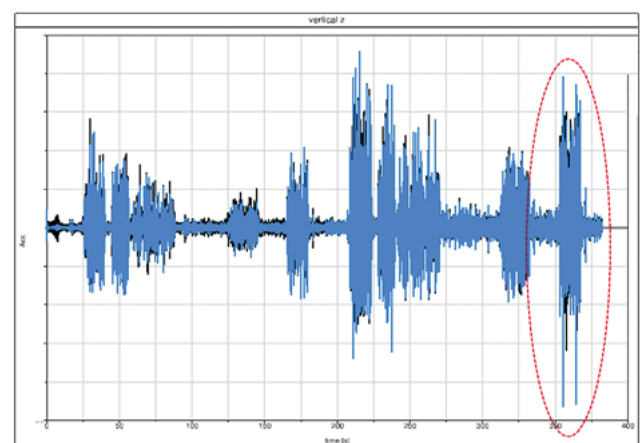


Fig. 8: Time history of vertical acceleration data | black - measured data, blue - simulated accelerations after second optimization

bushing values from the hydro-pulse (MBS simulation without parameter optimization)

- accelerations of the optimized simulations after identification of linear parts (red)
- accelerations of the optimized simulations after identification of nonlinear parts (blue).

The diagram of the measured and simulated vertical accelerations shows the very good fitting for medium and small amplitudes. Especially for large amplitudes, the result quality was significantly improved by incorporating the nonlinearity in the stiffness characteristic. The largest deviations existed in the track section “bad national road” for the empty truck (framed in red area), because this section was not taken into account in the identification loop of the nonlinear bushing characteristics. In retrospect, especially for the identification of nonlinear characteristics, all relevant road sections had to be considered in order to achieve quantitatively good results.

The representation in time domain, as shown above, can offer a rough overview, but a significant comparison criterion is missing. Classification methods, such as level crossing count (diagram below), allows a better evaluation of the quantitative comparison. The level crossing counting shows the important information regarding the number and the level of amplitudes. Only in the identification of the linear parts of the mount characteristics did the rare extreme amplitudes still show large deviations (red curve). However, the improvement in the adaptation of large amplitudes due to the identification of the nonlinear bump stops is clearly shown in the diagram below.

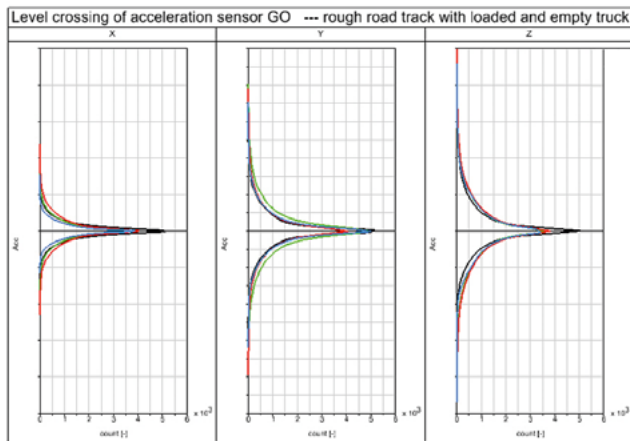


Fig. 9: Level crossing count | black - measured data, green - simulated accelerations with dynamic measurements of the mounts, red - simulated accelerations after first optimization, blue - simulated accelerations after second optimization

A good correlation of the maximum amplitudes concerning amount and number was, of course, extremely relevant for the durability calculations. Amplitudes which were smaller than 20% of the maximum amplitudes had a minor influence on durability.

A further contemplation was the calculation of the damage. The calculation of the damage provided a criterion that allowed the quantitative assessment and comparison

of curves with a single value. The damage calculation was done by assuming a ‘virtual’ fatigue life curve, so the damage values allowed a relative comparison.

The damage calculation of the measured and the simulated accelerations showed the efficient improvement of the optimization process carried out. The existing deviations were due to the unconsidered sections of the track and, of course, due to the assumptions made during model building.

Overall, there was a positive development of the calculated damage for each spatial direction. The efficiency of the developed optimization process was obvious. The variances in the damage could be qualified by the fact that even within several measured accelerations from rough road track, a deviation of 30% in the damage could be detected.

		pseudo damage	normalized damage
GO in X	Black	1.38E-15	1.00
GO in X	Green	8.30E-15	6.04
GO in X	Red	2.97E-15	2.16
GO in X	Blue	4.03E-16	0.29
GO in Y	Black	3.49E-14	1.00
GO in Y	Green	9.65E-14	2.77
GO in Y	Red	1.38E-13	3.96
GO in Y	Blue	3.90E-14	1.12
GO in Z	Black	8.07E-14	1.00
GO in Z	Green	3.62E-13	4.49
GO in Z	Red	2.58E-13	3.20
GO in Z	Blue	1.44E-13	1.78

Fig. 10: Table of pseudo damage | black - measured data from rough road track, green - simulated accelerations with dynamic measurements of the mounts, red-simulated accelerations after first optimization (linear section), blue - simulated accelerations after second optimization (non-linear section)

### Conclusion

The optimization strategy derived from this study utilized the fact that in some track sections the mounts acted exclusively in the linear parts of the stiffness characteristics. On the other hand, there were sections of the track where the mounts operated in the nonlinear part of the bushing characteristics. Only through targeted splitting of the complete track and the adaptation of an individual optimization strategy on the identification process, could a very good fitting for medium and smaller amplitudes be achieved. The high damage potential of large load amplitudes required a high correlation with the measurement. This balance must be considered by the incorporation of nonlinearity in the stiffness characteristic during the identification process. The largest deviation occurred in the section ‘bad road’ of the empty truck, because this section was not taken into account in the identification process of the nonlinear bushing characteristics. It was recommended that during the iden-

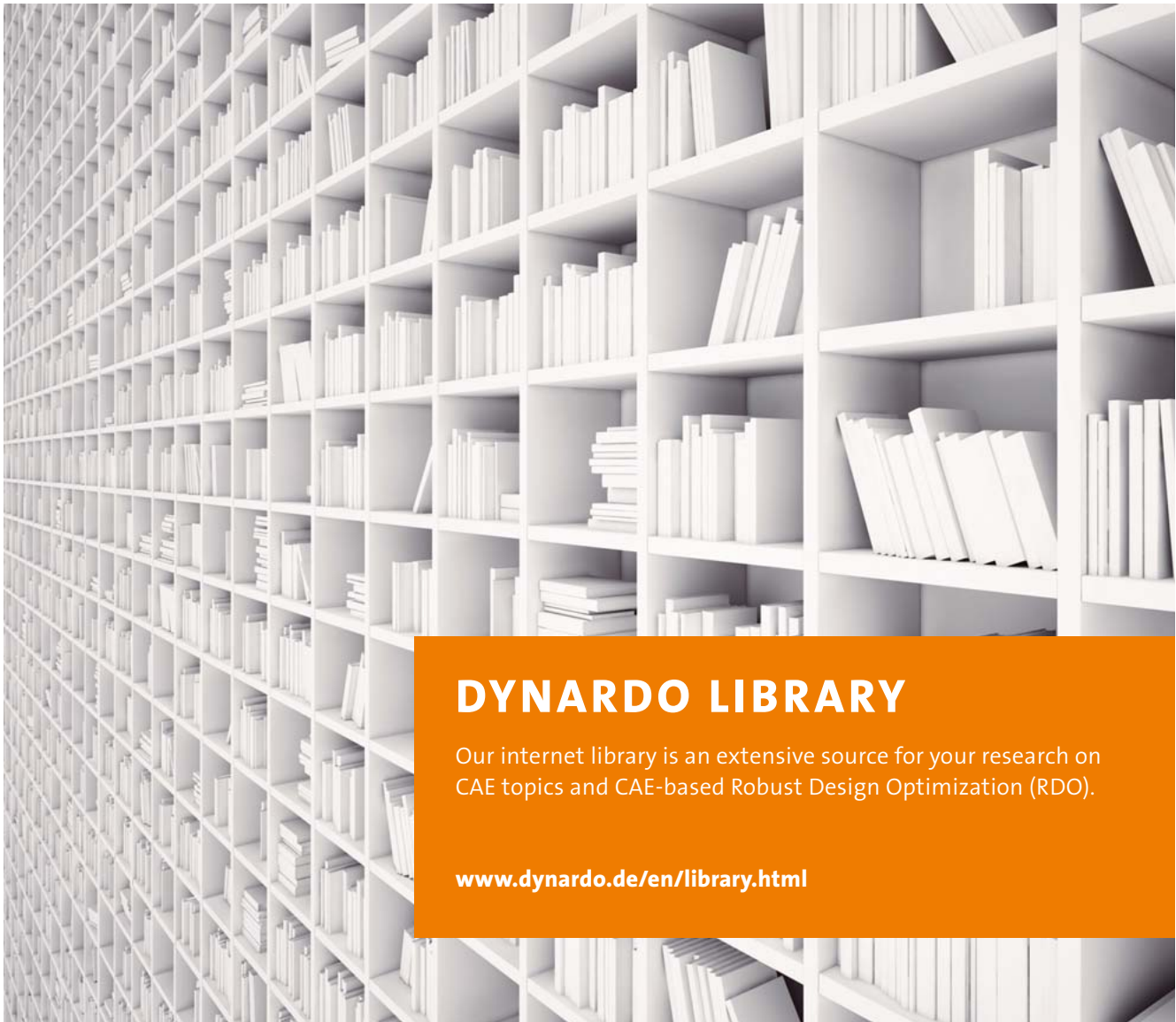
tification process, all sections with large amplitudes should have been considered in order to obtain quantitatively good results.

Overall, the methodology of automated parameter identification played an important part in the alternative load determination process for gearbox housings. For this purpose, it was necessary to derive a problem dependent, individually tailored optimization strategy in order to achieve the desired result. Only after the successful development of such a suitable process was it possible to generate quantitatively useful results for the calculation of durability. However, if the presented methodology shall be used for identifying load spectra for the component testing of gearbox housings, the results have to be robust and safe. Due to this and also for the generation of meaningful simulation models, parameters have to be scattered within their possible physical limits. The influence of scatter on the result must be exactly assessed.

In this way, reliable load limits for the design can be derived and defined. This next step can also be reached with the used optimization software in the existing process loop.

**Author //** A. Rasch (ZF Friedrichshafen AG)

**Source //** [www.dynardo.de/en/library](http://www.dynardo.de/en/library)



## DYNARDO LIBRARY

Our internet library is an extensive source for your research on CAE topics and CAE-based Robust Design Optimization (RDO).

[www.dynardo.de/en/library.html](http://www.dynardo.de/en/library.html)

## FE-MODEL GENERATION OF TURBOCHARGER BLADES REGARDING GEOMETRICAL TOLERANCES

With the help of optiSlang and SoS, realistic FE-models of turbine wheels as a part of small gasoline turbochargers were generated in order to analyze and to optimize their tolerance behavior.

### Introduction

The goal was to develop a fully automatized procedure to generate 3D-CAD geometries of turbocharger turbine wheels including different kinds of real production imperfections. The procedure incorporated the evaluation of particular deviations and differences from nominal blade geometry, hub body geometry and backface geometry. Since the turbine design was integrated, the blades and hub have been considered as a single part.

The wheel was manufactured by investment casting, so different sources of deviations were considered. Tool tolerances, casting process parameters, shrinking of wax and metal during solidification and cooling as well as finishing process steps had influence on the final geometry. Each geometrical feature, like massive hub body, thin blade body, machined or un-machined surfaces had different deviations. In the numerical system, the process of determination of deviations could be reproduced for many different virtual geometry designs and the space of the designs' deviations could be statistically evaluated. Based on these statistical evaluations, it could be stated with quantified probability in which interval ranges the geometrical deviations occurred.

The original numerical simulation process for turbine wheels design was split up into geometry generation and FEM analysis. Geometry generation needed to be parametrized to set up an automatized repeatable design generator. Utilizing a progressive technology of statistical metamodeling implicitly included in optiSlang, a statistical Metamodel of Optimal Prognosis (MOP) describing relations between input parameters (geometry modification) and output parameters (geometry deviations) could be established. Using such a statistical metamodel as a solver instead of a geometry generation process, the whole procedure could be increased rapidly.

The incorporation of virtual simulations of geometrical deviation into the process of turbocharger development had a certain positive impact on a better understanding of the deviation causes and deviation statistical properties. This knowledge led to a better performing turbocharger design and eliminated unnecessary tight tolerances. On the other hand, the robustness of several design features could be evaluated and improved.

### Contact-element based algorithm for tolerances evaluation

Algorithms for the evaluation of deviations represented the core of the whole process. Four different algorithms were designed to measure four different types of deviations. Assuming production deviations, it is necessary to measure the distances between external surfaces (see Fig. 1), thickness differences, curves and points distances. ANSYS classic environment was chosen for the implementation of algorithms ensuring robustness and a wide variability in customization. Contact and target finite elements (designed and derived in ANSYS for performing nonlinear structural analysis) were used to determine distances between the defined surfaces (gaps respectively penetrations in terminology of ANSYS). Based on this feature, differences between the nominal and design geometry were calculated and further processed. The results were available for all nodes of the FEM mesh, but it was advisable to pick a certain number of relevant nodes for the evaluation of production scatter. Interesting post-processing nodes might be located either on the edges that could be measured with tactile instruments or on topological points that could also be checked by optical measurement systems. To be able to understand the system behaviour, a reasonable amount of nodes needed to be selected intelligently. Full surface results were nevertheless an interesting source of information when selecting designs for further analysis. Through the use of numerical contact algorithms and distance calculation, they resembled the typical post-processing results of optical 3D scans.

### Process integration

As the core of the process was the deviation measuring techniques prepared in the classic environment of ANSYS, it was a crucial task to set up the process of gaining the devia-

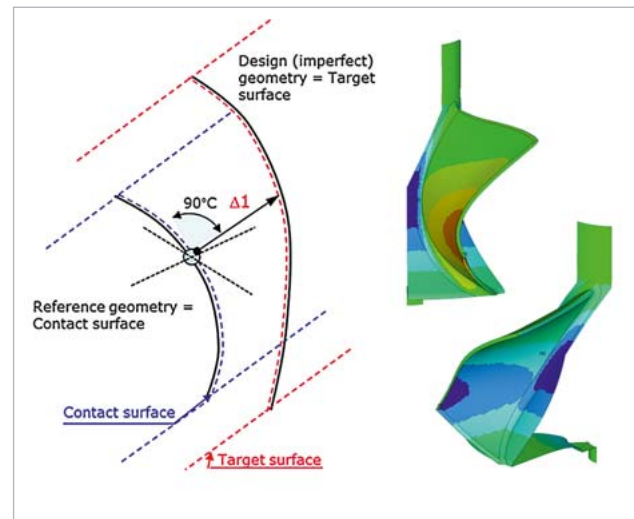


Fig. 1: Example of external surface deviations on the blade and hub body

tions from the moment of geometry creation in BladeGen and DesignModeler until the deviation of automatic value extraction. It was the only way to post-process the results from hundreds of different designs. Some design features like blade thickness were exclusively defined in BladeGen, while others like fillet radii were exclusively defined in DesignModeler. Both systems have their own interfaces and file formats. Also, in case of impossible geometries, different exit conditions had to be recognized. These inherent properties of the task made it necessary to have a generic control system for the numerical process chain. The key control system determining the time flow of the process is optiSLang4. It enabled the user to compose a sophisticated structure of particular actors representing the various actions that were supposed to happen during the flow run (see Fig. 2).

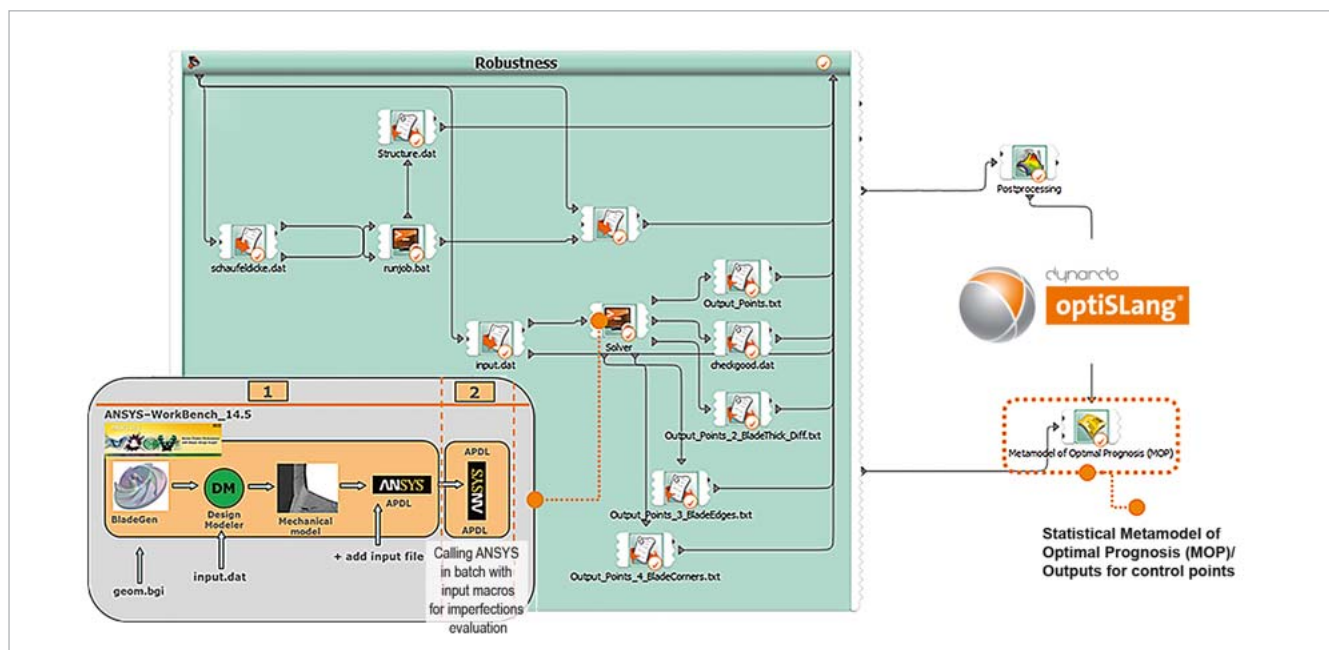


Fig. 2: Process flow in optiSLang

The process started with the creation of the correlated input set of parameters. Parameters were spatially correlated using the random fields' technique (see Fig. 3). Correlation dependencies designed by random fields secured that the geometrical deviations result in "reasonably" imperfed blade designs (see Fig. 3). Designed blade surfaces with higher density of surface waves were not in compliance with the produced turbochargers. Other parameters like blade length were generated randomly.

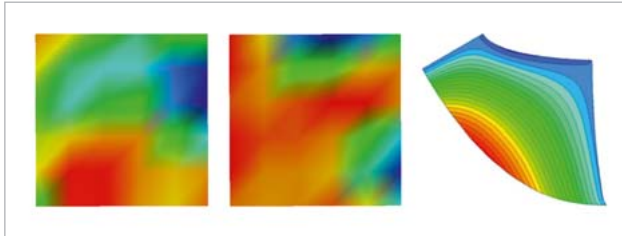


Fig. 3: Example of random fields' realizations (left), correlated thickness distributions (right)

After the preparations of input parameters, the main part of the process was started (see Fig.2 – main solver part). A new blade design was produced by BladeGen based on the correlated input parameters and other parameters passed on into the BladeGen tool. The blade was then finished in DesignModeler, connected to the hub body with a fillet radius, fitted with a backface and nose as well as prepared for exporting to ANSYS solver. Deviations were calculated using ANSYS and sent to optiSLang4 as responses. optiSLang4 evaluated the statistical quantities and created an MOP for the chosen responses.

### Strategy of producing non-nominal geometries

The process described in chapter 3 could be performed as a sensitivity (robustness) analysis. Results of such a procedure were the statistical quantities representing the dependencies between the input and output parameters. Since not all parameters of the geometry generation related directly to a length or position, it was useful to have a tool that quantified scatter of the actual measured feature versus the input parameter. This was necessary information when tuning the deviations to typical manufacturing

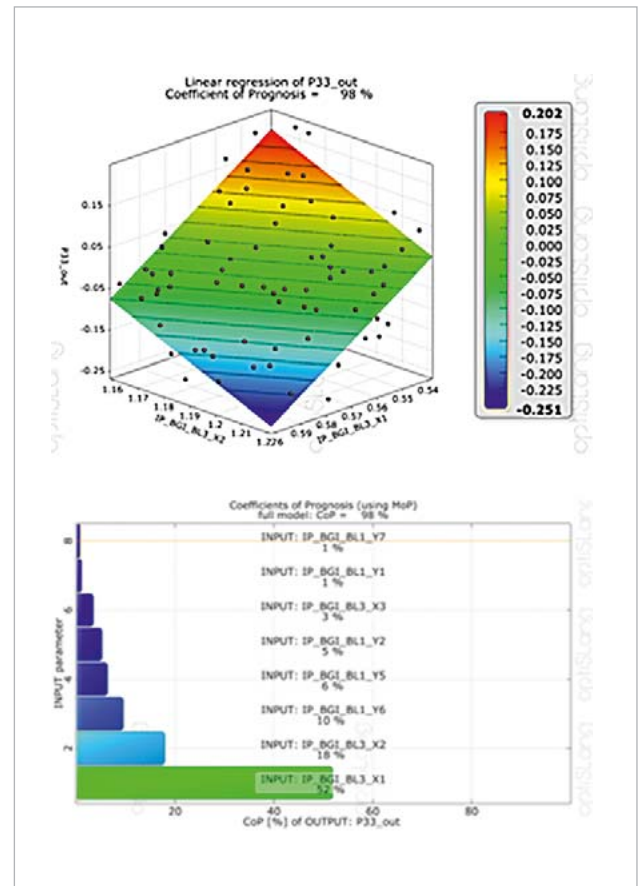


Fig. 4: MOP for the chosen response (top), Coefficient of Prognosis (bottom) The process flow integration was based on Windows and Python scripts.

values, especially when splines were used in geometry generation. Over these statistical quantities, the MOP could be created for more important purposes:

1. Quantification of the explainability of the output parameters.
2. Determination of the dependencies between input and output parameters.
3. Statistical verification of the deterministic procedure.
4. MOP could be used as a substitutive solver

Utilizing MOP as a solver, it was possible to calculate a sufficient amount of designs in a reasonable time. Designs calculated this way were cross-checked by the parallel per-

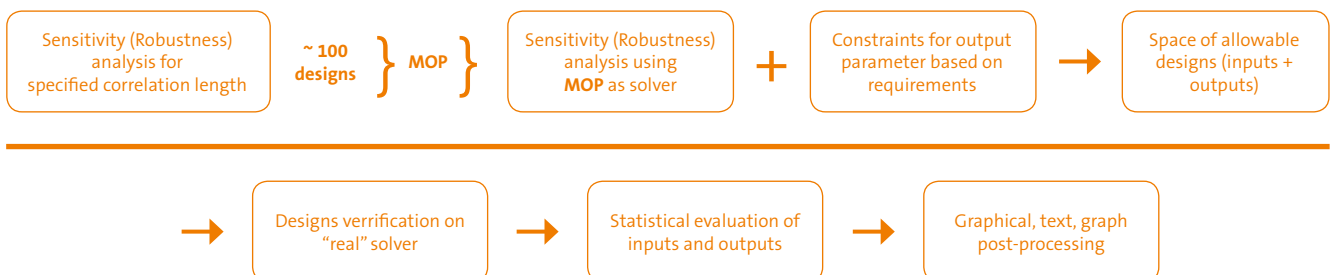


Fig. 5: Strategy for the evaluation of deviations

forming of the full process. After collecting all the responses, different response filters were applied to create a space of allowable designs.

### Sensitivity analysis

The sensitivity analysis provided basic statistical properties of the inspected problem. As a first step, a set of input and output parameters had to be defined. In between, the functional dependencies were expected. Using LHS, it was possible to cover the desired design space (within the input parameters' ranges) with a reduced number of samples (50-200, see Fig. 6).

An evaluation of structural mechanics of the non-nominal designs expected extreme cases to be the most interesting ones. Therefore, a non-centrally emphasized sampling was helpful. This was even more relevant when high nonlinearities were involved. The effect of one parameter might have been much higher in a border area of the design space than in the center or on the opposite side. Information about this could only be available when the sampling combined boundary values of several parameters at the same time. The higher the number of evaluated samples, the better quality of statistical properties was to be expected. The dependence of the number of input parameters was low, but with a number of around 50 input parameters, it was advisable to do at least 100 successful designs with LHS. To be able to achieve this, even under the presence of instabilities, a larger number was requested in optiSLang accordingly. The run could be aborted when the number of successful designs was reached. Performing sensitivity analysis, the following valuable information was provided:

1. Stability of designed process workflow (eventual manifestation of conflicts)
2. Relations between input and output parameters were determined
3. Utilizing the MOP on the design space, it was possible to determine the importance of the input parameters on each of the output parameters. Additionally, the participation of the input parameters was quantified. Dependencies determined between inputs and outputs could be highly non-linear as well.
4. Obtaining high values of Coefficients of Prognosis (CoP) for the responses, it is proven that defined responses can be well explained by the defined input parameters. In an opposite case the reasons for low values of CoPs should be considered. This way, the whole process was subjected to statistical verification.
5. MOP represents the mathematical dependencies between the inputs and outputs. Knowing these dependencies, it was possible to use such a statistical metamodel as a substitutive (significantly faster) solver. Results obtained from such a solver contain a certain error expressed by the CoP.

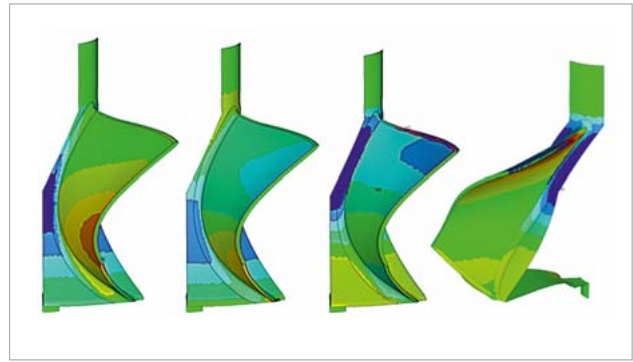


Fig. 6: Variability of the parameterization

Sensitivity analyses were successfully carried out either by using the whole designed procedure or using the MOP as a substitutive solver.

### Metamodel of Optimal Prognosis (MOP) as a generator of non-nominal geometries

The MOP is a statistical meta-model containing special features suitable for usage in a wide spectrum of probabilistic problems. As any statistical model, it is able to predict the values of responses with a certain quality of approximation. The prediction quality of an approximation model may be improved if unimportant variables are removed from the model. This idea is adopted in the MOP which is based on the search for the optimal input variable set and the most appropriate approximation model (polynomial or MLS with linear or quadratic basis). Due to the model independence and objectivity of the CoP measure, it is well suited to compare the different models in the different subspaces.

As it is possible to reach a high precision of the MOP (quantified by COP), it is very convenient then to use it as a substitutive solver representing dependencies between input and output qualities. In the case of the presented calculation process of a turbine wheel's deviations, it took about 25-30 minutes to complete one design containing unique geometry variation. The main fraction of this time was used for distance calculation between thousands of nodes. But the geometry generation in DesignModeler was also costly due to the interface with BladeGen on the one hand and 3D fillet generation on the other hand. After solving a sufficient amount of various wheel designs (in this case ca. 120) and building up the metamodel over the design space, it was stated that over 90% of the output parameters had a COP higher than or equal to 85% (see Fig. 4). Based on this knowledge, it was feasible to use the MOP as a substitutive solver with the expectation of obtaining a reasonable quality of results. Utilizing the MOP as a solver in the process workflow caused a dramatic acceleration of design generating performance. Compared to the full process workflow, the speed when using the MOP was more than 1000 times faster. Due to such an acceleration, it was possible to carry out sensitivity (robustness) analyses containing 2000 designs and more in less than one hour. This performance sig-

nificantly gained a higher amount of designs than it would be possible with only a full workflow. It brought to light valuable statistical information about the relations between the geometry variations and appropriate deviations.

### Filters

One of the consequences resulting from MOP utilization was the higher amount of produced output data. To get an overview of design scatter, many ways of data post-processing exist. Histograms of frequencies of occurrence (Fig. 7) can be displayed for each of the output parameters. Each histogram can be approximated by the best-fitting type of statistical distribution. Once the statistical distribution was attributed, the probability of response occurrence in a specified continuous interval could be easily determined. Sorting the output of designs according to the chosen criteria was a way to aggregate the result information from the whole design space. In optiSlang4, it is convenient to use the constraint conditions feature in order to sort or to filter the designs according to ranges of response. Intending to implement a filter which will sort out all the designs having at least one of the responses (from a selected set of appropriate responses) out of a given interval (symmetric, defined by bound =  $\beta$ ), it is necessary to set up the following conditional constraining equations for all involved responses:

$$ABS(Value_{Desing}) \leq Value_{required} \rightarrow ABS(P18\_OUT\_Th\_Diff) \leq \beta$$

$$\rightarrow ABS("all other related responses") \leq \beta$$

By the application of the formerly described filter on the design space, only the designs fulfilling the conditions for all the responses remained. The others were considered to be invalid. The primary deficiency of this basic filtering technique was the fact that a design could only be valid (status=1) or invalid (status=0). Furthermore, neither the amount of responses that violated the allowable bounds for each design nor their extent of violation was known. In order to obtain

this information for the estimation whether the violation was only local or occurred at a larger area, it was necessary to create a new actor in optiSlang4 that contained a Python function summing up the violations for each design. The advantage was a deeper insight into the probability of the occurrence of limit violations. An example of another useful filter is the “two belts filter”. Also, a certain tolerance on the allowed deviations of 20% was introduced. The purpose of this filter was to sort out all the designs with responses outside the two defined intervals (see Fig. 8).

$$\rightarrow ABS(\text{All related responses}) \geq 0.8 \times \beta \wedge (\text{All related responses}) \leq 1.2 \times \beta \wedge (\text{All related responses}) \geq -1.2 \times \beta$$

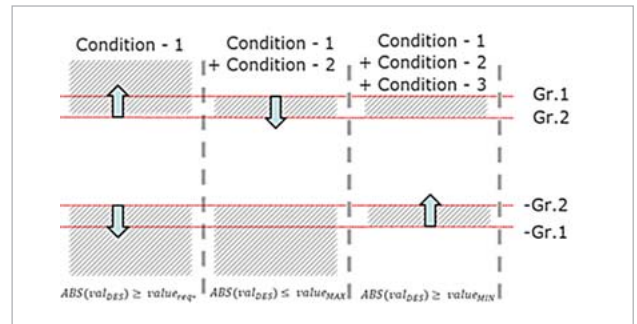


Fig. 8: Example of “two belts filter”

The filters based on constraining equations could be implemented either in the GUI, using predefined interface, or in Python scripts that could be prepared in advance and later on be inserted in optiSlang4. The opportunity of using Python scripts at any moment of creation of an optiSlang4 workflow enabled a preparation of a higher amount of responses, conditions, parameters etc.

**Author //** Dr. B. Lehmayr (Continental Automotive GmbH) / M. Mrozek, Dr.-Ing. R. Schlegel (Dynardo GmbH)  
**Source //** [www.dynardo.de/en/library](http://www.dynardo.de/en/library)

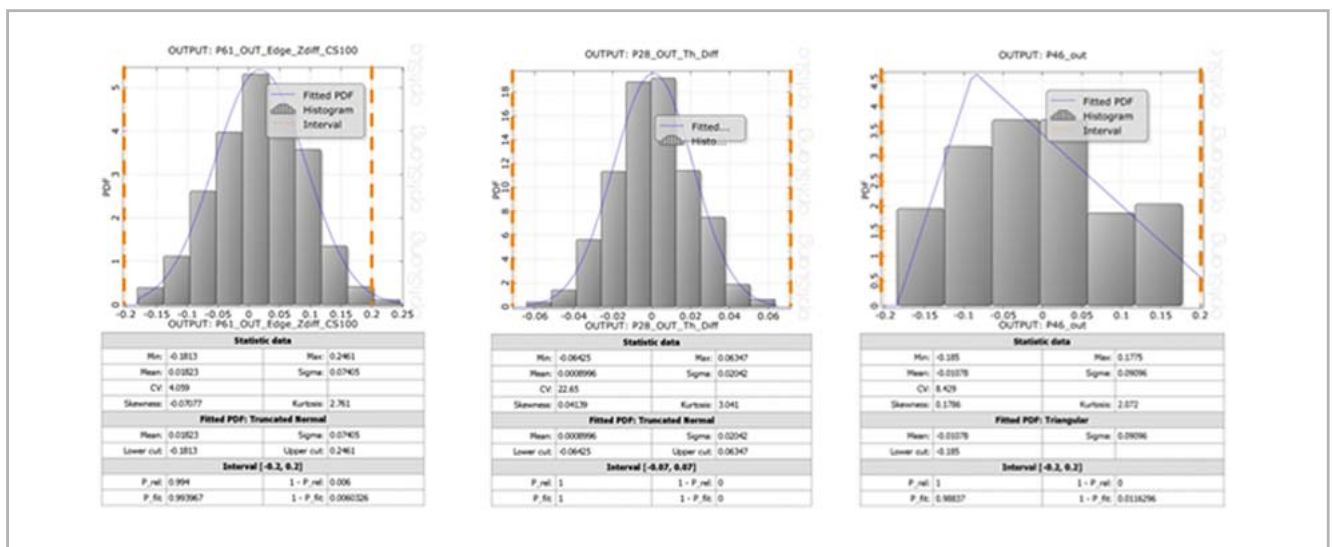


Fig. 7: Statistical distribution of attribution



## ANNUAL WEIMAR OPTIMIZATION AND STOCHASTIC DAYS

Your conference for CAE-based parametric optimization, stochastic analysis and Robust Design Optimization in virtual product development.

The annual conference aims at promoting successful applications of parametric optimization and CAE-based stochastic analysis in virtual product design. The conference offers focused information and training in practical seminars and interdisciplinary lectures. Users can talk about their experiences in parametric optimization, service providers present their new developments and scientific research institutions inform about state-of-the-art RDO methodology.

Take the opportunity to obtain and exchange knowledge with recognized experts from science and industry.

You will find more information and current dates at:  
[www.dynardo.de/en/wosd](http://www.dynardo.de/en/wosd).

We are looking forward to welcoming you to the next Weimar Optimization and Stochastic Days.



CUSTOMER STORY // AUTOMOTIVE ENGINEERING

## ROBUST DESIGN OPTIMIZATION ENSURES HIGH-QUALITY WINDOW MECHANISMS

**Brose uses optiSLang to evaluate design alternatives of window regulators. The simulation procedure includes manufacturing variations and verifies the robustness for a wide variety of car models.**

### Introduction

To be able to feel the wind in your hair while driving your car, pay the fee for parking in a lot, or grab takeout coffee from the drive-through, you need a window regulator. This device is a part that moves a window in automobile doors up and down on command. Brose, the world's largest manufacturer of window regulators, builds these components for many vehicle models. The same basic regulator must work for a wide range of curved window sheet radii, serve the three different positions of a wedge that is used to adjust the windows to the chassis of the car, account for stiffness variations of several components, and adapt to variations in the torque used to assemble the regulator. On rare occasions, these variables have interacted to generate excessive stresses, strong enough to crack the window glass. Brose used robust design optimization (RDO) to evaluate a series of design alternatives against the huge number of possible combinations of application variables based on stress levels in the glass. RDO eliminated the need to simulate each combination of variables by generating a meta-model used to explore the complete design space in a fraction of the time. The simulation helped the Brose team to understand the cause of cracking; it also made it possible to optimize the design for

robustness needed to accommodate a wide variety of car models and to withstand manufacturing variations. Brose is the world's fourth largest privately held automotive components supplier. The company supplies 52 million window regulators a year to many of the world's leading automobile manufacturers. Brose has achieved this leadership position by providing a compact design, which reduces assembly costs, along with motors that deliver a high performance-to-cost ratio. The company ensures high economies of scale and low piece costs by using standard components produced in high volumes. For Brose to continue its good reputation, these components must operate reliably under all expected conditions.

### Complex ways of application factor interaction

A key component of the window regulator is the clamp plate/rail slider assembly that attaches to the window and must adjust to fit curved windows, whose radius ranges from 900 mm to 2,000 mm. The rail slider and clamp plate are connected by a screw that penetrates the glass. The assembly applies pressure to both sides of the glass to hold

it in place; this generates shear stress due to the window's curvature. A wedge between the glass and the rail slider can be adjusted to one of three positions to maintain sealing pressure between the glass and the car chassis. The Young's modulus of the rail slider and clamp plate can differ due to manufacturing variation. The amount of torque that is applied to the screw during assembly is not always exactly the same. These factors interact in complex ways. One result is material damage that sometimes occurs when the screw is tightened during the assembly process.



Typical Brose window regulator

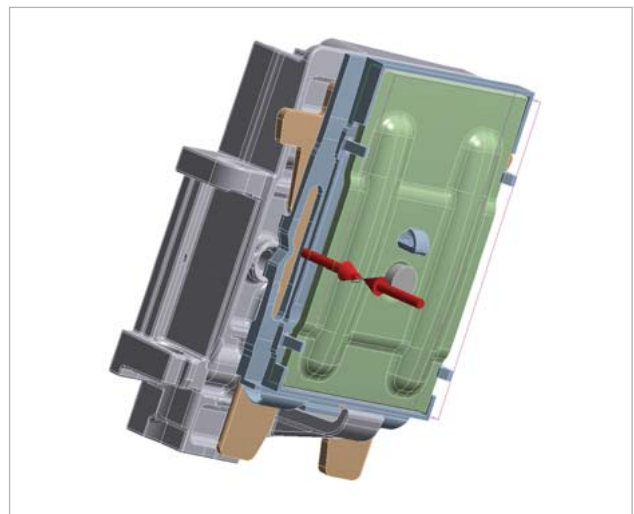
The Brose Group worked with Dynardo's optiSLang software to address this problem. Dynardo developed optiSLang as the basis for RDO in virtual product development; the company also offers consulting services. Brose engineers modeled the clamp plate/rail slider assembly in ANSYS Mechanical to evaluate the slider's current design and to manually change the model for different application conditions. With a few manual runs, engineers were able to generate excessive stresses in the glass that correlated well to the areas that broke during the assembly process. These runs validated the ability of finite element analysis to accurately reproduce the problem. But the huge number of possible combinations of different variables made it impossible to validate a potential solution using manual analysis techniques.

### Parameterizing the model

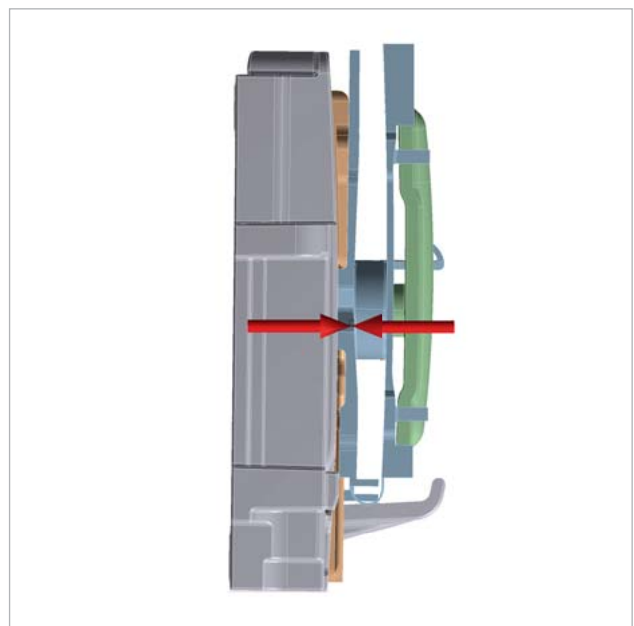
To determine a more robust solution, Brose engineers defined eight input parameters in the ANSYS Workbench environment, including the wedge position, window radius, Young's modulus of the rail slider and clamp plate, and pretension of the screw used to assemble the rail slider and clamp plate.

Engineers varied an additional seven geometric input parameters to represent design changes to the window radius and clamp slider. The team defined seven key finite element analysis results, including maximum stress in window, stress at the hole in the glass, stress at the bottom edge of the glass, and contact pressure of the slider to the window.

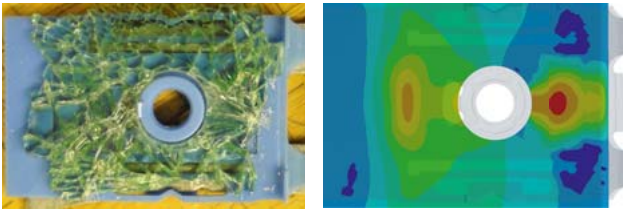
The large number of design variables involved in this problem result in such a large number of possible design points that it would be impractical to comprehensively explore with current computing power. To address this challenge, optiSLang was used to calculate the meta-model, or simplified model of the design space, that provides the best approximation of the complete space. This meta-model, called the Metamodel of Optimal Prognosis (MOP), was utilized to calculate the optimal design with much less computing power.



CAD model of clamp plate and rail slider assembly



Clamp plate and rail slider assembly applies stress to glass. The arrows represent the bolt



Left: Area of actual cracked window surrounding screw hole | right: Stress analysis results correlate well with actual window component

Brose engineers applied optiSLang to configure a designed experiment using Latin hypercube sampling to scan the multidimensional space of input parameters. Approximately 120 design points were selected that, as a whole, provide a good approximation of the complete design space. optiSLang drove ANSYS Mechanical to solve each of these design points in parallel on a high-performance computing cluster running ANSYS Mechanical. The engineers used optiSLang to construct an MOP based on these 120 samples, which was used to approximate the complete design space in a small fraction of the clock time and computational effort that would be required to explore the complete design space.

### Identifying key application factors

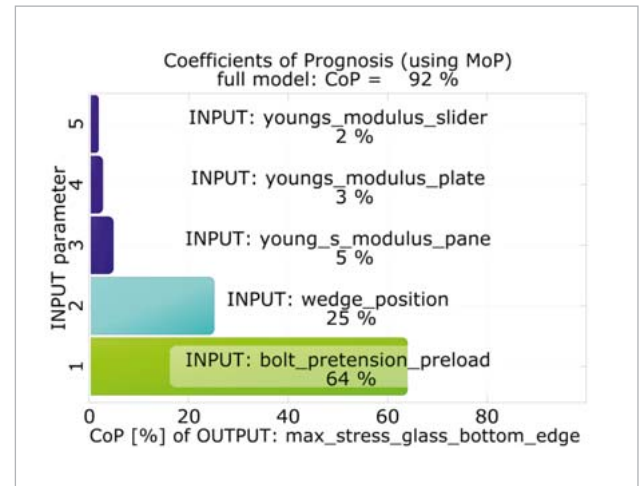
As part of generating the MOP, optiSLang automatically identified the most important application factors with respect to their impact on window stresses. The optimization software quantified the forecast quality of many global meta-models and selected the MOP with the best predictive power. Then optiSLang calculated the coefficient of prognosis (CoP), which quantifies the ability of the MOP to accurately predict the complete design space. The CoP of 0.92 indicates that the MOP can be used to produce accurate estimates of performance of proposed designs over the complete design space.

As it created the MOP, optiSLang also performed a sensitivity analysis that identified the most important input parameters in terms of influence on output variables. This analysis showed that the bolt pretension preload has the most impact on the stress of the window and that the wedge position has the second-greatest influence. Brose engineers mapped the maximum stress in the glass, the most important response, as a function of these two critical variables, expecting to gain a visual understanding of the root cause of the problem. The response surface maps showed the interaction of these variables and identified combinations of values with the potential to cause excessive stresses.

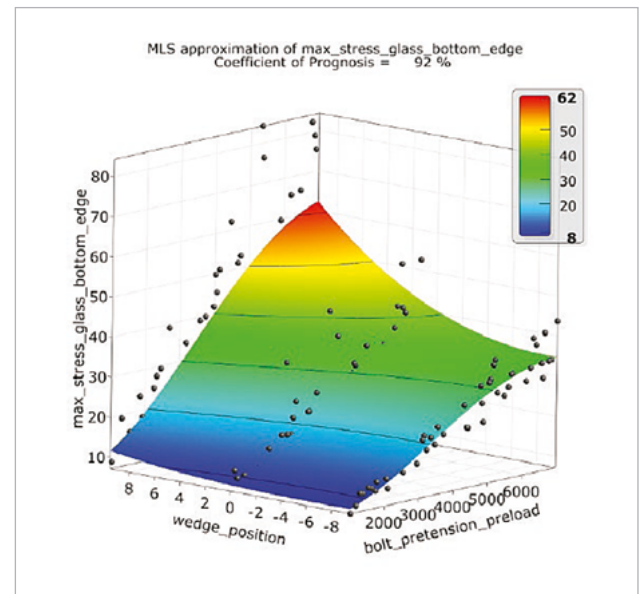
### Optimizing the design

Brose engineers optimized the design based on their engineering experience. Then they evaluated the new design with the MOP to be sure that every combination of the input parameters generated less than the maximum allowable stress on the glass. The CoP validated the MOP's predic-

tive power and indicated that the new design would keep stress levels well within acceptable values throughout the complete design space. Simulation tools from ANSYS and Dynardo have helped the Brose product development team to identify the most sensitive design parameters for the window mechanisms and to optimize these parameters to further improve quality over a wide range of applications.



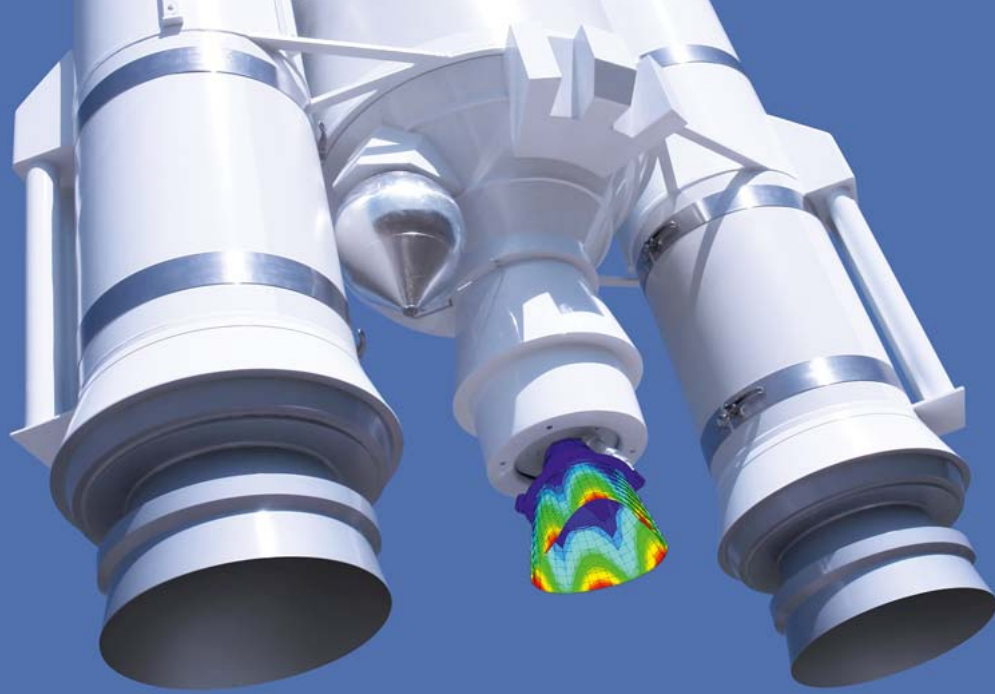
Metamodel indicated which variables had the greatest impact on window stress



Response surface map shows stress as a function of key variables for initial design

**Author //** Th. Sauernheimer (Brose)

This article originally appeared in ANSYS Advantage magazine.



CUSTOMER STORY // AEROSPACE INDUSTRY

## FATIGUE VERIFICATION OF HIGH LOADED BOLTS OF A ROCKET COMBUSTION CHAMBER

Sensitivity analyses and robustness evaluations with optiSLang including dynamic load conditions during flight operation help to verify high quality standards of bolt connections.

### Introduction

Rocket engines and the bolted interfaces between their components have to withstand intense thermal and structural loads. Therefore, particular emphasis is placed on the quality assurance and verification from incoming inspection of the fasteners. During these tests, a fatigue analysis is performed to ensure a high bolt durability covering the dynamic loads during the engine's operation. However, there is a significant difference between test and flight loads leading to a non-linear relation between test results and expected operational life. A sensitivity analysis is conducted to generate a linking, multi-parametrical model that can be adapted to both load cases. While the parameters scatter within the unifying parameter set, the life expectation also varies for both load cases. Accordingly, a robustness analysis is finally performed to project the result variety under flight conditions onto the test result scattering.

Bolts or screws connect constructional parts with each other. The threaded bolt shaft and its evenly shaped counterpart nut or threaded blind hole transmit forces by a shapeclosed connection. In the case of overloading, the bolt will fail and lose its force transmitting capability.

A bolt can be overloaded by stressing leading to ductile failure, preferably at the first thread in contact. Another overloading mechanism is known as critical fatigue after the exposure to a certain number of load cycles. The second will be outlined in this article.

### Basics on bolt analysis

#### Pretension

During bolt mounting into a blind hole or a nut, pretension has to be generated. Continuous torque tightening increases bolt and flange force at the same rate, while the value of deformation depends on the stiffness of both components. Due to the tension load, the bolt is strained by the law of elasticity  $\Delta l_B = F_B / K_B$  with the bolt force  $F_B$  and the bolt's rigidity  $K_B$  that leads to the absolute bolt deformation  $\Delta l_B$ . With the same force  $F_B$  but a different flange stiffness  $K_F$ , the flange parts are compressed about  $\Delta l_F = F_B / K_F$ . Here  $\Delta l_F$  denotes the deformation of the flange area in an imaginary cylinder between the bolt head and the nut.  $K_F$  is the corresponding flange stiffness.

The mounted and pre-stressed interface is loaded by the operational force  $F_L$ . If  $F_L$  is oriented in tension direction, the bolt will be additionally stressed while the flange compression decreases. Hence the operational load is taken by both components depending on their stiffness. The ratio between the force fraction taken by flange decompression  $F_{LF}$  and the part covered by the bolt  $F_{LB}$  is defined by the force ratio  $\Phi$ :

$$\Phi = \frac{K_B}{K_B + K_F} = \frac{F_{LB}}{F_L} \quad (1)$$

The bolt and flange behavior due to pretension and operational load is illustrated in Figure 1.

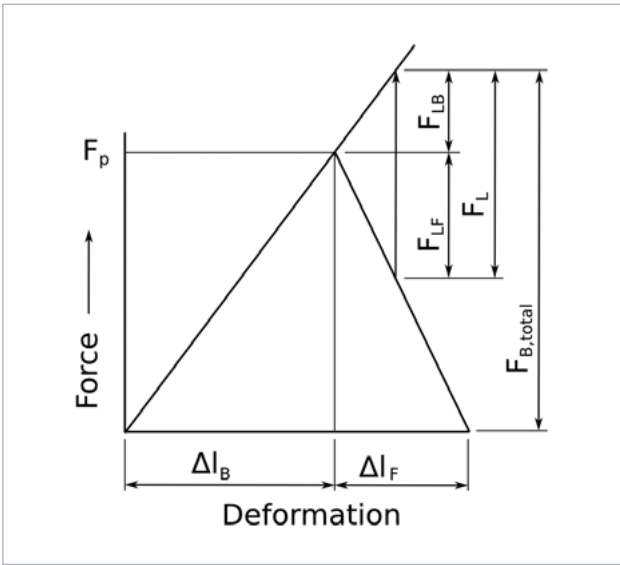


Fig. 1: Load-deformation-curve of a classical bolt connection

The effect of the force ratio becomes substantial for dynamic loading domains. The high durability of bolted joints is to be attributed to  $\Phi$  and the fact that an operational load is partly taken by the relief of the pre-stressed flanges. The higher the flange stiffness compared to the stiffness of the bolt shaft, the lower the actual impact on operational loads stressing the bolt. This effect is related to equation (1). This advantageous behavior decreases the bolt stress range per cycle which crucially increases the bolt life.

### Stress distribution

Loaded by an axial force  $F_{ax}$ , the nominal stress  $\sigma_{nom}$  within the bolt shaft equals to:

$$\sigma_{nom} = \frac{F_{ax}}{A_{st}} \quad (2)$$

with  $A_{st}$  as stress area.

Notch effects at the thread ground lead to a local stress concentration  $\sigma_{max} = K \cdot \sigma_{nom}$ . The stress concentration factor  $K$  depends, among other things, on the depth of the

thread and the radius of the thread ground. To estimate the magnitude of  $K$ , tables are presented in engineering literature, e.g. Young and Budynas [2002]. As a result of the stress concentration at the thread grounds, a stress distribution equivalent to Figure 2 occurs.

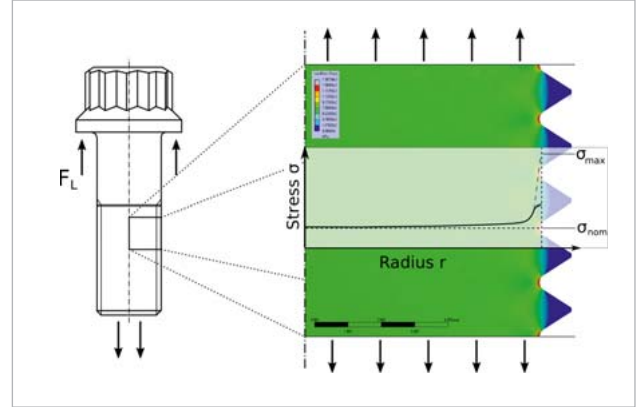


Fig. 2: Stress distribution along threaded bolt and stress concentration at thread grounds

When the locally increased stress reaches the yield limit  $\sigma_y$ , local plastic deformations occur. For this study, the Neuber rule is used to approximate the magnitude of plastic deformation. Neuber expects a hyperbola in the stress-strain field where the generation of stress and strain stays constant  $\sigma \varepsilon = \sigma_{max}^2/E$ . When the Neuber hyperbola fits the endpoint of the linear extrapolated stress-strain line  $\sigma_{max,el}$ , it crosses the yield curve at the point  $\sigma_{max,Neuber}$ . This point approximates the stress-strain relation after yielding as shown in Figure 3. As a yield curve, a bilinear approximation is used. It is defined by the yield limit  $(R_{p0.2}/E, R_{p0.2})$  at ultimate conditions  $(A, R_M)$ .

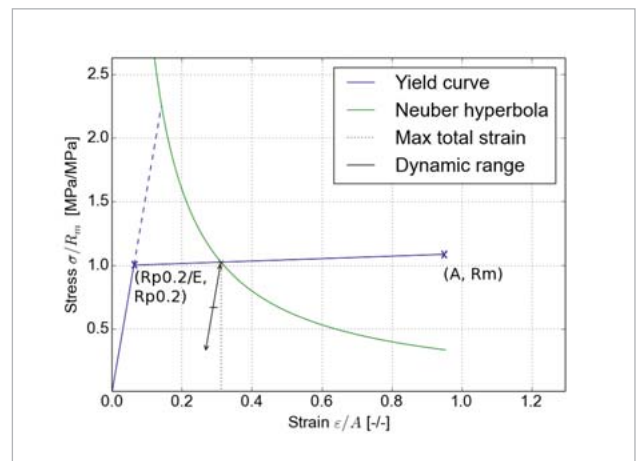


Fig. 3: Plastic stress-strain state obtained by Neuber approximation

### Fatigue damage

The bolt life prediction is realized by the Coffin Manson approach. With the universal slope proposed by Lemaitre and Chaboche [1990]:

$$\begin{aligned}\Delta\varepsilon_{\text{univ.}} &= f(N_f) \\ &= 3.5 \frac{R_m - \sigma_m}{E} \cdot N_f^{-0.12} + D_u^{0.6} \cdot N_f^{-0.6}\end{aligned}\quad (3)$$

the total strain range  $\Delta\varepsilon$  is related to the number of cycles until failure  $N_f$ .  $R_m$  being the ultimate strength,  $D_u$  is the ductility of the material and  $\sigma_m$  is the mean stress of the load cycle.

Herein, the values in the exponents are fitted to a wide range of different materials for universal validity. To reach our needs, these constants are considered as material specific and are chosen in accordance to the bolt material. A better adjustable form of (3) is used with the parameters  $C_1$  to  $C_4$  that can be fitted to the actual material behavior:

$$\begin{aligned}\Delta\varepsilon &= f(N_f) \\ &= C_1 \frac{R_m - \sigma_m}{E} \cdot N_f^{-C_2} + D_u^{C_3} \cdot N_f^{-C_4}\end{aligned}\quad (4)$$

Aligned values for  $C_1$  to  $C_4$  can be found for different materials in Lemaitre and Chaboche [1990]. Varying the constants  $C_1$  to  $C_4$  of (4), it influences the  $\Delta\varepsilon - N_f$ -Curve as shown in Figure 4. The actual sensitivity of the model towards these Coffin Manson parameters is analyzed in section 4.

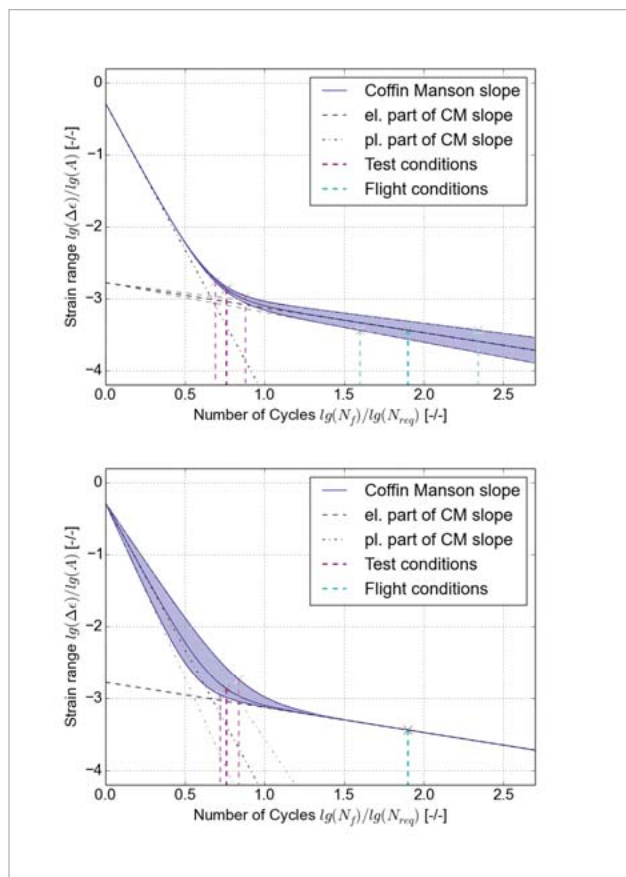


Fig. 4: Coffin Mansons fatigue curve - variety of the constants  $C_2$  and  $C_4$  are shown by the diffuse bluish areas

## Bolt validation procedure and uncertainties

To accept the bolts for flight application, a few per batch are submitted to several different test procedures. The check regarding fatigue failure is performed by a cycling test. It is known that the load conditions during the test differ to those experienced during the rocket launch. The objective of this investigation was to correlate the results of the fatigue test with the circumstances of real operation. Finally, it had to be shown that the required cycles during the flight can be validated by a certain number of test cycles.

### Validation test conditions

For fatigue testing, the bolt was inserted into the testing device with contact at the thread and bolt head. No flange material was considered. Loads applied by the device were fully covered by the bolt itself. The full range of alternating testing loads were applied to the bolt. The diagram in Figure 5a (see next page) displays the load-deformation curve of this behavior.

The large load range of  $2F_a$  combined with the stress concentration factor at the thread ground lead to a local cyclic plasticification as shown in Figure 2. According to the Neuber approximation, this opened the stress-strain hysteresis, stretched the stress range and reduced the bolt life significantly.

### Flight conditions

The considered bolts connect the combustion chamber to the injector. During mounting, a high pretension  $F_p$  was applied to avoid interface sliding. The dynamic interface loads  $F_L$  occurred in a moderate level which lead to a relatively low alternating bolt force  $F_a$  compared to the pretension force  $F_p$ . The ratio can be seen in the load deformation curve in Figure 5b (see next page). With high flange stiffness, which was given in this case, the dynamic loads added to the pretension were mostly covered by flange relief. The actual bolt load  $F_a$  alternated in a much smaller stress range compared to the test case. That lead to a solely elastic dynamic behavior with a lesser strain range. According to Coffin Manson and shown in Figure 4, a small  $\Delta\varepsilon$ - resulted in a significantly longer bolt life than under test conditions.

### Correlation of test results to flight conditions

To compare test results with flight live expectations, the mentioned influences needed to be considered. Slight uncertainties of yield stress  $R_{p0.2}$  and strain at rupture  $A$  lead to contrary changes in the calculation of the strain range via the Neuber approximation approach. This exceeded the resulting live expectation. Additional uncertainties occurred by varying the Coffin Manson coefficients  $C_1$  to  $C_4$ . Also, the stress concentration factor of the threat  $K$  was not a definite value but depended on geometrical width ratio and the edge radius which was not definitely detectable. It was treated as a variable during the following investigations.

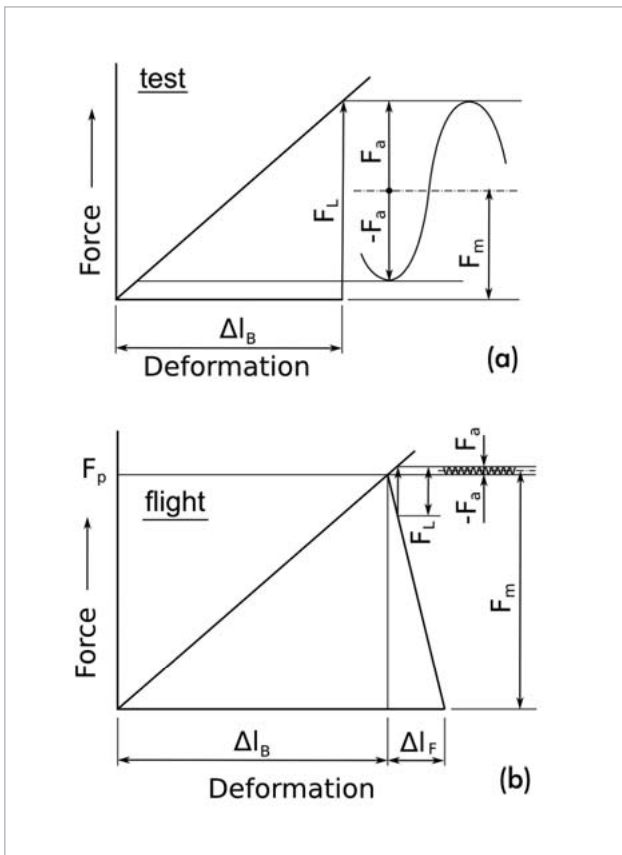


Fig. 5: Load-deformation-curve under a) test conditions and b) flight conditions

Life expectations were calculated by considering a certain set of the mentioned variables. Each parameter set had two results:

- $N_{f,test}$  – life expectation under test conditions and
- $N_{f,flight}$  – life expectation during the flight

Finally, it had to be shown that the flight requirement was reached in all cases, which meant in any possible combination of input variables. Parameter combinations that lead to lower life expectation needed to be excluded by the choice of the test conditions.

### Robustness under flight conditions

All possible variables influencing the bolt’s life expectation were analyzed. After performing a sensitivity analysis with optiSLang, it could be seen that the influence of parameters varied from flight to test case. The test case showed the highest sensitivity to the Coffin Manson variables  $C_1$  and  $C_2$  that were responsible for the high cycle domain of the slope.

For the flight case, these variables had a minor impact. Despite to its small strain range  $\Delta\varepsilon_{flight}$ , the sensitivity was mostly strength driven.  $R_{p0.2}$  and  $R_m$  were the most influencing parameters in this case. Table 1 lists the sensitivities for both cases.

Parameter	unit	Test	Flight
$A_m$	[%]	0	1
$E$	[MPa/MPa]	0	0
$K$	[%]	1	4
$R_{p0.2}$	[MPa/MPa]	9	36
$R_m$	[MPa/MPa]	16	58
$C_1$	[%]	47	3
$C_2$	[%]	17	5
$C_3$	[%]	1	0
$C_4$	[%]	6	0

Table 1: Model sensitivity under test and flight conditions towards input parameters

Considering the influencing parameters as normally distributed, the model was fed with specific parameter sets. The distribution of the parameters was evaluated from test data, or, in the case of the Coffin Manson variables, from literature. For each input set, an output of the two life expectations was obtained – one for test and one for flight.

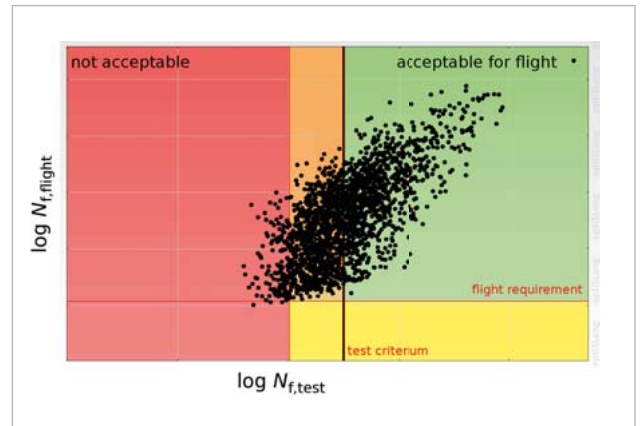


Fig. 6: Criteria for fatigue test

With optiSLang, a robustness analysis was executed. As a result of the life evaluation, the plot shown in Figure 6 was drawn. It shows the life results of 5000 parameter sets. For each set, the expected flight life was prognosticated for a calculated test life. As a requirement for flight acceptance, the bolts had to withstand the specified loads, even with the worst possible combination of material parameters. As shown in Figure 6, all points below the flight requirements were not accepted meaning all test results in the red area would lead to bolt rejection from flight worthiness. If one of the few tested bolts per incoming batch showed an unacceptable fatigue durability, the whole batch was not allowed to be mounted.

The actual test requirement was finally defined at a higher number of cycles during the test to meet an additional safety factor. Test results in the orange area (see Figure 6) could achieve acceptance level by performing additional analysis. The big plus of the indifferent orange area was the early recognition of any disadvantageous changes of production methods. If processes changed, the final product could be affected in a negative way. With the demanding test requirement, changes could be detected early and counteractions could be prepared.

The bolts that met the test requirement, illustrated by the green area in Figure 6, were accepted for flight without further analysis.

The acceptance regarding bolt life could finally be verified. With the possibility of taking all parameters into account within a single analysis, the understanding of its sensitivities was improved. Having the bandwidth of each parameter in mind, the spread of the bolt life expectation could be shown. In the anthill plot shown in Figure 6, this life expectation was projected on the durability under testing conditions. With the relations between flight and test, a new test criteria was found that disqualified unacceptable bolts before they went to flight.

**Author //** Marcus Lehmann, Dieter Hummel  
(Airbus Defence & Space)

**Literature //** Jean Lemaitre and Jean-Louis Chaboche. Mechanics of solid materials. Cambridge university press, 1990./ Warren Clarence Young and Richard Gordon Budynas. Roark's formulas for stress and strain, volume 7. McGraw-Hill New York, 2002.



## DYNARDO TRAININGS

**At our trainings, we provide basic or expert knowledge of our software products and inform you about methods and current issues in the CAE sector.**

### Info Days and Webinars

During our info days and webinars, you will receive an introduction to performing complex, non-linear FE-calculations using optiSlang, multiPlas, SoS and ETK. At regular webinars, you can easily get information about all relevant issues of CAE-based optimization and stochastic analysis. During an information day, you will additionally have the opportunity to discuss your specific optimization task with our experts and develop first approaches to solutions.

### Trainings

For a competent and customized introduction to our software products, visit our basic or expert trainings clearly explaining theory and application of a sensitivity analysis, multidisciplinary optimization and robustness evaluation. The trainings are not only for engineers, but are also perfectly suited for decision makers in the CAE-based simulation field. For all trainings there is a discount of 50% for students and 30% for university members/PHDs.

### Info

You will find all information as well as an overview of the current training program at:

[www.dynardo.de/en/trainings](http://www.dynardo.de/en/trainings)

## Contact & Distributors

### Germany & worldwide

Dynardo GmbH  
Steubenstraße 25  
99423 Weimar  
Phone: +49 (0)3643 9008-30  
Fax.: +49 (0)3643 9008-39  
www.dynardo.de  
contact@dynardo.de

Dynardo Austria GmbH  
Office Vienna  
Wagenseilgasse 14  
1120 Vienna  
www.dynardo.at  
contact@dynardo.at

### Germany

CADFEM GmbH  
Marktplatz 2  
85567 Grafing b. München  
www.cadfem.de

science + computing ag  
Hagellocher Weg 73  
72070 Tübingen  
www.science-computing.de

### Austria

CADFEM (Austria) GmbH  
Wagenseilgasse 14  
1120 Wien  
www.cadfem.at

### Switzerland

CADFEM (Suisse) AG  
Wittenwilerstrasse 25  
8355 Aadorf  
www.cadfem.ch

### Czech Republic, Slovakia, Hungary

SVS FEM s.r.o.  
Škrochova 3886/42  
615 00 Brno-Židenice  
www.svsfem.cz

### Sweden, Denmark, Finland, Norway

EDR & Medeso AB  
Lysgränd 1  
SE-721 30 Västerås  
www.medeso.se

### United Kingdom of Great Britain and Northern Ireland

IDAC Ltd  
Airport House Business Centre  
Purley Way  
Croydon, Surrey, CR0 0XZ  
www.idac.co.uk

### Ireland

CADFEM Ireland Ltd  
18 Windsor Place  
Lower Pembroke Street  
Dublin 2  
www.cadfemireland.com

### Turkey

FIGES A.S.  
Teknopark Istanbul  
Teknopark Bulvari 1 / 5A-101-102  
34912 Pendik-Istanbul  
www.figes.com.tr

### North Africa

CADFEM Afrique du Nord s.a.r.l.  
Technopôle de Sousse  
TUN-4002 Sousse  
www.cadfem-an.com

### Russia

CADFEM CIS  
Suzdalskaya 46, Office 203  
111672 Moscow  
www.cadfem-cis.ru

### India

CADFEM Engineering Services India  
6-3-902/A, 2nd Floor, Right Wing  
Rajbhawan Road, Somajiguda  
Hyderabad 500 082  
www.cadfem.in

### USA

CADFEM Americas, Inc.  
27600 Farmington Road, Suite 203 B  
Farmington Hills, MI 48334  
www.cadfem-americas.com

Ozen Engineering Inc.  
1210 E Arques Ave 207  
Sunnyvale, CA 94085  
www.ozeninc.com

### USA/Canada

SimuTech Group Inc.  
1800 Brighton Henrietta Town Line Rd.  
Rochester, NY 14623  
www.simutechgroup.com

### Japan

TECOSIM Japan Limited  
4F Mimura K2 Bldg. 1-10-17  
Kami-kizaki, Urawa-ku, Saitama-shi  
Saitama 330-0071  
www.tecosim.co.jp

### Korea

TaeSung S&E Inc.  
Kolon Digital Tower 2  
10F, Seongsu-dong 2 ga  
Seongdong-gu  
Seoul 333-140  
www.tsne.co.kr

### China

PERA-CADFEM Consulting Inc.  
Bldg CN08, LEGEND-TOWN  
Advanced Business Park,  
No. 1 BalizhuangDongli,  
Chaoyang District,  
Beijing 100025  
www.peraglobal.com

## Publication details

### Publisher

Dynardo GmbH  
Steubenstraße 25  
99423 Weimar  
www.dynardo.de  
contact@dynardo.de

### Executive Editor & Layout

Henning Schwarz  
henning.schwarz@dynardo.de

### Registration

Local court Jena: HRB 111784

### VAT Registration Number

DE 214626029

### Publication

worldwide

### © Images

Fotolia: P. Palazzi, p. 10 | H. Bogdan, p. 22 | PRILL Mediendesign, p. 25

### Copyright

© Dynardo GmbH. All rights reserved

The Dynardo GmbH does not guarantee or warrant accuracy or completeness of the material contained in this publication.